NACA

RESEARCH MEMORANDUM

ANALYSIS OF TWO-SPOOL TURBOPROP-ENGINE CHARACTERISTICS

By Elmer H. Davison

Lewis Flight Propulsion Laboratory
Cleveland, Ohio

NATIONAL ADVISORY COMMITTEE
FOR AERONAUTICS

WASHINGTON

June 3, 1957

NACA RM E57C21

NATIONAL ADVISORY COMMITTEE FOR AERONAUTICS

RESEARCH MEMORANDUM

ANALYSIS OF TWO-SPOOL TURBOPROP-ENGINE CHARACTERISTICS

By Elmer H. Davison

SUMMARY

Two-spool turboprop engines with an over-all compressor pressure ratio of 12 split 6-2, 3-4, and 2-6 between the outer and inner compressors were analytically investigated for a range of turbine-inlet temperatures and flight conditions.

The 2-6 engines, in comparison with the 6-2 engines, are restricted in the range of turbine-inlet temperature for which they can be designed if turbine stator adjustment in the outer turbines is not employed. The use of turbine stator adjustment makes the turbine design requirements more difficult and, in general, does not appreciably reduce the specific fuel consumption. Compressors of advanced design can be employed without encountering severe turbine stress limits. For engine operation without turbine stator adjustment, the 2-6 engines require the greatest range of outer-compressor operation. The operating line for the inner compressor of the 6-2 engines is nearly vertical (small change in equivalent weight flow), while that for the 2-6 engines nearly parallels the surge line. The design stress, frontal area, and pressure ratio for the outer turbine increase considerably with altitude and flight speed for operation with constant exhaust-nozzle area. It appears desirable, therefore, to employ an adjustable exhaust-nozzle area that can be closed down at altitude to avoid these increases. The design requirements of the inner turbines are not affected to any extent by the flight condition.

The variations of specific fuel consumption with turbine-inlet temperature are considerably less than for single-spool engines (investigated previously) of comparable compressor pressure ratio. Comparison of two-spool engines with single-spool and free-turbine engines (investigated previously) revealed that increasing the pressure ratio obtained in the outer compressor of a two-spool engine results in characteristics similar to those of a single-spool engine, while reversing the split results in characteristics similar to those of a free-turbine engine. Comparison of the two-spool and single-spool engines, for those aspects investigated herein, does not reveal any major limitations or differences which clearly indicate that one type is inherently better than the other.

INTRODUCTION

An analytical investigation of the performance characteristics and the design problems of turboprop engines has been conducted at the NACA Lewis laboratory. Some of the turbine design problems encountered in a single-spool engine with current compressor pressure ratio (7.32 at design) were investigated in reference 1. The investigation was extended in reference 2 to cover the effect of mode of engine operation on the turbine design requirements and engine performance for a single-spool engine with current compressor pressure ratio. In reference 3, single-spool engines and free-turbine engines utilizing a single-spool compressor with high compressor pressure ratio (14.4 at design) were investigated.

The trend in turboprop engines is to higher compressor pressure ratios and higher turbine-inlet temperatures, because the result is lower specific fuel consumption and higher specific power. The two-spool engine is of interest because it offers one means of obtaining the higher compressor pressure ratios desired. The purpose of this report is to present the results of an analytical investigation of the engine characteristics of two-spool engines with high over-all compressor pressure ratio (12.0 at design).

The following facets of the two-spool engine were investigated: the relative sizes of the engine components from compressor inlet to tailcone outlet, some of the aerodynamic characteristics of the compressor and turbine combinations, the turbine stress characteristics, the effect of turbine-inlet temperature and flight condition on the engine component requirements, and the sfc and engine power characteristics. The two-spool engines of this investigation were also compared with single-spool and free-turbine engines investigated previously.

In this study an over-all design compressor pressure ratio of 12 was assigned. Engines with this over-all compressor pressure ratio of 12 split 6-2, 3-4, and 2-6 between the outer and inner compressors were investigated. The actual rotative speed of the outer compressor for all engines was held constant for all flight and operating conditions. The following three flight conditions were investigated for a range of turbine-inlet temperature from 1600° to 2600° R:

(X) Sea-level static

(Y) Flight velocity 400 mph, altitude 19,000 feet

(Z) Flight velocity 600 mph, altitude 40,000 feet

Turbine stator adjustment was also considered. The two configurations investigated were (1) outer-turbine stator adjustment alone and (2) outer- and inner-turbine stator adjustment in combination.

ANALYSIS

In the previous analyses of single-spool and free-turbine engines (refs. 1 to 4), the effects of such things as mode of engine operation, turbine-inlet temperature, and flight condition on the engine characteristics have been established. Many of the conclusions obtained in these previous analyses pertaining to single-spool and free-turbine engines apply to two-spool engines. When the present analysis was initiated, it was thought that the division of the over-all compressor pressure ratio between the outer and inner compressors would perhaps be the most important additional consideration in delineating the design problems and features of the two-spool engine. Therefore, in this investigation an over-all design compressor pressure ratio of 12 was assigned; and engines were investigated with this over-all pressure ratio split 6-2, 3-4, and 2-6 between the outer and inner compressors.

The analysis is of the type wherein hypothetical compressor performance maps are used with assumed constant turbine efficiencies to determine the turbine design requirements and their effect on other engine requirements. The engine performance characteristics were also investigated. A schematic diagram of a two-spool turboprop engine with station locations is shown in figure 1, and compressor performance maps are given in figure 2. Symbols used herein are defined in appendix A.

In appendix B, the analytical procedure followed in obtaining a series of figures (e.g., figs. 3 to 8) for each compressor-pressure-ratio split is explained. The four main assumptions made in constructing these figures are as follows:

(1) The rotative speed of the outer compressor is constant.

(2) The ratio of exhaust-nozzle area to outer-compressor frontal area is constant at 1.4.

(3) The adiabatic efficiencies of both the inner and outer turbines are constant at 0.85.

(4) Stator adjustment is permitted in the outer but not the inner turbine.

From these figures it is possible to determine the effects of compressor-pressure-ratio split, turbine-inlet temperature, and flight condition on many of the turbine design requirements, engine performance, and compressor operating characteristics. The parameters investigated are plotted against the total-pressure ratio across the inner turbine p_4'/p_5' (see fig. 1) in order to determine whether it might be desirable to incorporate turbine stator adjustment in the outer turbine. With no stator adjustment in the outer turbine the pressure ratio p_4'/p_5', as

shown in appendix B, is constant for all flight conditions and turbine-inlet temperatures. The case of no stator adjustment (p_4'/p_5' = const.) can thus be easily compared in the figures presented with the case of stator adjustment in the outer turbine.

Stator adjustment for both the inner and outer turbines was considered, but only a discussion of the results is presented. The additional reduction in specific fuel consumption sfc that could be obtained by using stator adjustment in both turbines, rather than only in the outer turbine, was negligible. Also, the engine could be operated over the range of turbine-inlet temperature assigned with stator adjustment in the outer turbine alone; and, therefore, employment of stator adjustment in the inner turbine appeared to be a needless complication.

Figure 9 shows the interrelation of inner-turbine centrifugal stress and various compressor aerodynamic and geometric parameters for the sea-level static condition at a turbine-inlet temperature of 2100° R. The derivations of figures 9(a) to (f) are given in appendix B. These figures were used to select the equivalent design speeds and frontal areas of the inner compressors. The centrifugal stresses in the last rotors of the inner turbines are, for the equivalent design speeds and frontal areas selected, within a 1000-hour stress-rupture limit for an HS-31 blade material when the turbine-inlet temperature is 2100° R. Table I lists for the various compressors the equivalent design speeds, frontal areas, and so forth. An explanation of these selections is given in appendix B. The outer compressors for all three compressor-pressure-ratio splits had transonic inlet stages with design relative inlet Mach numbers at the tip of the first rotor of 1.2. The inner compressors had design relative inlet Mach numbers at the tip of the first rotor of 0.8, 1.0, and 1.2 for the 6-2, 3-4, and 2-6 compressor-pressure-ratio splits, respectively.

Selection of an optimum engine from the figures discussed in this section would depend to a large extent upon the importance attached to individual requirements. These figures were used to examine in this report the effect of compressor-pressure-ratio split, turbine-inlet temperature, and flight condition on engines having no stator adjustment in either turbine and engines that obtain minimum sfc by use of stator adjustment in the outer turbine.

Figure 10 presents the variations in outer-turbine-inlet equivalent weight flow $w\sqrt{\theta_5'}/\delta_5'A_{t,1}$, outer-turbine total-pressure ratio p_5'/p_6', inner-turbine total-pressure ratio p_4'/p_5', ratio of outer-turbine-exit to outer-compressor-inlet frontal areas $A_{t,6}/A_{t,1}$, ratio of inner-turbine-exit to outer-compressor-inlet frontal areas $A_{t,5}/A_{t,1}$, outer-turbine-exit blade centrifugal stress $S_{b,6}$, inner-turbine-exit blade

centrifugal stress $S_{b,5}$, ratio of engine power to outer-compressor-inlet frontal area $P^*/A_{t,1}$, and specific fuel consumption sfc with turbine-inlet temperature T_4' and flight condition for the three compressor-pressure-ratio splits. Only exit stresses are considered for the turbines, since they are usually a reliable guide to the severity of the turbine stress problem, even though blade rows forward of the last rotor might be stress-limited when the exit blade rows are not.

The curves are presented for the following two types of engines:

(1) Engine A: No stator adjustment in either turbine, and ratio of exhaust-nozzle area to outer-compressor frontal area of 1.4

(2) Engine B: Minimum sfc obtainable by using stator adjustment in outer turbine, and ratio of exhaust-nozzle area to outer-compressor frontal area of 1.4

The curves for engines A were obtained by cross-plotting, for example, from figures 3 to 8 for a 2-6 compressor-pressure-ratio split at a constant value of p_4'/p_5'. The curves for engines B were obtained by cross-plotting from figures 3 to 8 the values corresponding to the minimum sfc values of figure 5.

The compressor operating conditions for engines A are shown on the compressor performance maps (figs. 2(e) and (f)). These operating lines were obtained with the aid of figures 3 and 4. The other compressor-pressure-ratio splits were handled in the same manner.

RESULTS AND DISCUSSION

The engines with compressor-pressure-ratio splits of 3-4 have characteristics between those of the 6-2 and 2-6 compressor-pressure-ratio splits. Therefore, only engines with compressor-pressure-ratio splits of 6-2 and 2-6 are compared herein, with the implication that the 3-4 engines are midway between these extremes.

Effect of Compressor-Pressure-Ratio Split and Turbine Stator Adjustment

Turbine-inlet temperature. - Without turbine stator adjustment (engines A), the 2-6 engine (fig. 10(c)) in comparison with the 6-2 engine (fig. 10(a)) is restricted (usually by the compressors) in the range of turbine-inlet temperature over which it can be designed to operate. For example, the 2-6 engine can operate over a range of temperature from 1600° to only 2400° R at flight condition Z, whereas the 6-2 engine can

operate over a range of temperature from 1600° to 2600° R. The reason for this restriction is apparent from figure 5, which shows that, for a constant p_4'/p_5', design points at only a limited number of temperatures can be obtained for the 2-6 engine. For engines A of figures 10(b) and (c) (3-4 and 2-6 engines), the p_4'/p_5' cross-plot values were selected to give the greatest range of turbine-inlet temperature T_4' without sacrificing too much with respect to sfc. Some of the maximum and minimum T_4' values for the 3-4 and 2-6 engines shown in figures 10(b) and (c) may not be realistic, since they result in compressor operating conditions very near surge or at equivalent compressor operating speeds greater than those considered in constructing the compressor maps. For the 6-2 engine it was possible to select a p_4'/p_5' value that would give nearly minimum sfc and reasonable compressor operating conditions at all T_4' values.

The range of turbine-inlet temperature can be increased by using turbine stator adjustment (engines B). However, this results in more critical turbine design requirements, particularly for the 2-6 engine. Figure 10(c) shows that the outer turbines for engines B must be able to operate over a larger variation in inlet equivalent weight flow $(w\sqrt{\theta_5'}/\delta_5' A_{t,1})$ and that the percent change of pressure ratio p_5'/p_6' is greater than for engines A.

Specific fuel consumption. - The reduction in specific fuel consumption obtained by using turbine stator adjustment is usually quite small. Figure 10 shows that lower values of sfc can be obtained for the 2-6 engines than for the 6-2 engines at the lower turbine-inlet temperatures, but that little difference exists at the higher temperatures. Using stator adjustment in both the inner and outer turbines produces only slightly lower sfc for the three compressor-pressure-ratio splits than stator adjustment in the outer turbine alone or no stator adjustment in the 6-2 engines.

Centrifugal stress. - In calculating the exit centrifugal stress $S_{b,5}$ for the inner turbine, it was specified that the stress be well within a 1000-hour stress-rupture limit for an HS-31 blade material at flight condition X (sea-level static) and a turbine-inlet temperature of 2100° R. For engines A and a 6-2 pressure-ratio split (fig. 10(a)), the exit stress $S_{b,5}$ is nearly constant with turbine-inlet temperature and flight condition. Therefore, the turbine-inlet temperature could be raised to approximately 2300° R before exceeding the 1000-hour limit, since the design stress at a turbine-inlet temperature of 2100° R is well within a 1000-hour stress-rupture limit. The stress variations for engines A with a 2-6 pressure-ratio split (fig. 10(c)) are less favorable, because the exit stress $S_{b,5}$ increases with turbine-inlet temperature.

However, the stress could be held relatively constant by using turbine stator adjustment (engines B). The outer-turbine-exit centrifugal stress $S_{b,6}$ at flight condition X and a turbine-inlet temperature of 2100° R was also well within a 1000-hour stress-rupture life (see fig. 9(f)) for an A-286 blade material (ref. 5). Flight condition has a large effect on the exit centrifugal stress $S_{b,6}$, as is discussed subsequently.

Some of the compressor design requirements specified in order to obtain the stress values shown in figure 10 are given in table I. Except for the inner compressor of the 6-2 engine, all the compressors considered have transonic inlet stages; and even the inner compressor of the 6-2 engine is an advanced design by present standards. If lower turbine stresses are desired, they can be obtained by lowering the design tip speeds specified; but this reduction would increase the number of compressor and turbine stages required.

4301

Turbine frontal areas. - Figure 10(a) shows that the frontal areas of the inner turbines of the 6-2 engines are relatively small. This might result in some difficulty in obtaining smooth flow transition from the combustor outlet to the outer-turbine inlet. However, as pointed out in appendix B, this is considered a minimum area, since a 0.6 hub-tip radius ratio was assigned at the exit of the turbine. This frontal area can be increased (without increasing turbine stress) by assuming a larger hub-tip radius ratio. If the area ratio $A_{t,5}/A_{t,1}$ were increased to 1.0, for example, the hub-tip radius ratio would be 0.89. (The manner in which $A_{t,5}/A_{t,1}$ varies with hub-tip radius ratio is given by eq. (B33).) There is, therefore, some freedom of choice as to the area ratio $A_{t,5}/A_{t,1}$ to be used. The minimums are shown in figure 10, while the maximum area ratios would be determined by the maximum hub-tip radius ratio or minimum length blades that might be acceptable. The centrifugal stress would, in most instances, probably be held to a minimum by designing the turbines near limiting loading, which in turn tends to minimize the turbine frontal area (see appendix B). There is still some freedom of choice in the hub-tip radius ratio as mentioned, however, so that acceptable wall contours from the combustor outlet to the outer-turbine inlet should be obtainable. Increasing the frontal area of the inner turbine has the added advantage of increasing the blade speed, which in turn tends to ease the turbine aerodynamic design problem for a given number of stages or to reduce the required number of stages for given aerodynamic limits.

Compressor operating conditions. - The compressor operating conditions for engines A for the three compressor-pressure-ratio splits are shown in figure 2. The 2-6 engines require the greatest range of outer-compressor operation. The operating line for the inner compressor of the 6-2 engine is nearly vertical, while that for the 2-6 engine nearly parallels the surge line.

Effect of Turbine-Inlet Temperature

Compressor operating conditions. - The effect of turbine-inlet temperature on the compressor operating conditions for engines A can be seen in figure 2. Lowering the turbine-inlet temperature drives all the outer compressors toward surge. Raising the turbine-inlet temperature drives the inner compressor of the 6-2 engine toward surge and a region of lower efficiency at high pressure ratio. Raising the turbine-inlet temperature does not drive the inner compressor of the 2-6 engine toward surge, because the operating line nearly parallels the surge line, but does drive it into a region of lower efficiency at high pressure ratio and weight flow. (It should be noted that the outer compressor must operate very near the compressor surge limit for the 2-6 engines in order to design for turbine-inlet temperatures as low as 1600° R. For the highest temperature considered, 2600° R, the inner compressor must operate at equivalent compressor operating speeds higher than those considered in constructing the compressor maps.)

Power output, specific fuel consumption, and stress. - Figures 10(a) and (c) show that, for either compressor-pressure-ratio split, the power output $P^*/A_{t,1}$ varies nearly linearly with turbine-inlet temperature, and that sfc is nearly constant except for temperatures below 2000° R. Also, for engines A the turbine stress problem is more critical for the 2-6 compressor-pressure-ratio split than for the 6-2, because the stresses increase more rapidly with turbine-inlet temperature. The stress problem can be alleviated at higher temperatures by using turbine stator adjustment (engine B), but this makes the turbine design problems more difficult, as noted previously.

Effect of Flight Condition

Stress, frontal area, and pressure ratios. - Design stress and frontal area of the outer turbine for compressor-pressure-ratio splits of 6-2 and 2-6 increase with altitude and flight speed for operation at constant exhaust-nozzle area (figs. 10(a) and (c)). The pressure ratio across the outer turbine p_5'/p_6' also increases with altitude and flight speed. These variations can be eliminated with little effect on engine sfc by using an adjustable exhaust-nozzle area that is closed down as altitude and flight speed increase.

The increase in stress with altitude for operation at constant exhaust-nozzle area is accompanied by a reduction in blade-metal temperature for a constant turbine-inlet temperature T_4', since the pressure ratio across the outer turbine p_5'/p_6' increases with altitude. On a design-point basis, therefore, these higher stresses might be tolerated.

If an engine were designed for the altitude condition, however, the same stress would prevail at the sea-level static condition for the operation at constant outer-compressor speed specified herein. This high stress could easily exceed the stress-rupture limit at the sea-level static condition, since the outer-turbine pressure ratio p'_5/p'_6 is lower and consequently the turbine-exit temperature is higher. It thus appears advisable with respect to turbine stress also to incorporate exhaust-nozzle-area adjustment.

The other advantages stemming from the use of an adjustable exhaust-nozzle area are (1) a reduction in the frontal area of the outer turbine, which is the greatest frontal area for the engine proper, (2) a reduction in the range of pressure ratio over which this turbine must be designed to operate, and (3) as a consequence of the foregoing, a reduction in the number of turbine stages required. (It should be noted that the stresses $S_{b,6}$ and area ratios $A_{t,6}/A_{t,1}$ shown in fig. 10 are for turbines designed at limiting loading with exit hub-tip radius ratios of 0.6. If the turbines were designed with more conservative aerodynamic limits and larger exit hub-tip radius ratios, higher stresses and larger frontal areas would result, as pointed out in appendix B.) Thus, it is concluded from the analysis that high-performance compressors can be employed in the two-spool engines investigated without encountering severe turbine stress limits if an adjustable exhaust-nozzle area is used. It also appears as previously mentioned that, without turbine stator adjustment, the inner-turbine stress characteristics of the 6-2 engines are more favorable than those of the 2-6 engines.

Turbine efficiency. - In analyzing the engines, it was assumed that the turbine efficiency was constant for all operating conditions. This assumption appears valid for the inner turbines of engines A, since the turbine operating conditions (see figs. 10(a) and (c)) do not vary much with flight condition or turbine-inlet temperature. For the same reasons, the outer turbines for engines A should have reasonably constant turbine efficiency if exhaust-nozzle-area adjustment is employed to reduce the range of pressure ratio over which the turbines must operate. For engines B or operation with constant exhaust-nozzle area, however, the turbine efficiency will vary some with engine operating conditions, because the turbine operating conditions also change. For these engine types, one probably would design the turbine to have peak efficiency at the most important operating condition (perhaps the cruise condition) and accept lower turbine efficiency, and consequently higher sfc, at the other operating conditions.

Compressor operating conditions. - The effects of flight condition on the compressor operating conditions of engines A are shown in figure 2. The increase in flight speed and altitude tends to drive both the inner and outer compressors for all three compressor-pressure-ratio

splits into less favorable operating regions. The reductions in compressor efficiencies tend to be offset, however, by the increased cycle efficiencies resulting from the higher compressor pressure ratios.

Comparison with Single-Spool and Free-Turbine Engines

The variation of sfc with turbine-inlet temperature for a given flight condition for the two-spool turboprop is quite small (fig. 10) and is considerably less than for a single-spool engine of comparable compressor pressure ratio. This results primarily from the manner in which the compressor operating conditions change with turbine-inlet temperature.

The outer turbine of the two-spool engine, like the turbine in the single-spool engine and the free turbine in the free-turbine engine, has large variations in design frontal area, centrifugal stress, and pressure ratio with flight condition for operation with constant exhaust-nozzle area. For all engines it appears desirable to use an adjustable exhaust-nozzle area that can be closed down at altitude if high-altitude and high-flight-speed operation is contemplated.

Increasing the pressure ratio obtained in the outer compressor of a two-spool engine results in characteristics similar to those of a single-spool engine, while reversing the split results in characteristics similar to those of a free-turbine engine. This is best illustrated by the fact that the 6-2 engines without turbine stator adjustment are not limited in the range of turbine-inlet temperature for which they can be designed, whereas the 2-6 engines are limited. This parallels the conclusion drawn for the single-spool and free-turbine engines in reference 3. This would appear to be almost axiomatic, since the limiting compressor-pressure-ratio splits of 12-1 and 1-12 represent single-spool and free-turbine engines, respectively.

Comparison of the two-spool engines analyzed herein with the single-spool engines of references 1 to 3 does not reveal any major limitations or differences which clearly indicate that one type is inherently better than the other. Other aspects not considered (such as mechanical differences or acceleration characteristics) might be of paramount importance in selecting one engine in preference to the other, but such considerations are not within the scope of the present investigation.

CONCLUSIONS

Two-spool turboprop engines with an over-all design compressor pressure ratio of 12 split 6-2, 3-4, and 2-6 between the outer and inner compressors were analyzed. The following conclusions were reached:

1. The characteristics of the 3-4 engines are roughly midway between those of the 6-2 and 2-6 engines.

2. The 2-6 engines in comparison with the 6-2 engines are restricted in the range of turbine-inlet temperature for which they can be designed if turbine stator adjustment is not employed in the outer turbine.

3. If turbine stator adjustment is employed, however, more difficult turbine design requirements result.

4. In general, the reduction in specific fuel consumption obtainable with the use of turbine stator adjustment is small.

5. The stress problem for the inner turbine is less critical for the 6-2 than for the 2-6 engines, because the centrifugal stress for the inner turbine is essentially constant with increasing turbine-inlet temperature. However, the stress in the inner turbine of the 2-6 engines can be held relatively constant by using stator adjustment in the outer turbine.

6. Compressors of advanced design can be employed without encountering severe turbine stress limits if an adjustable exhaust-nozzle area is employed. Turbine stresses well within a 1000-hour stress-rupture limit for a turbine-inlet temperature of 2100° R can be obtained with the compressor designs contemplated.

7. For engine operation without turbine stator adjustment, the 2-6 engines require the greatest range of outer-compressor operation. The operating line for the inner compressor of the 6-2 engines is nearly vertical (small change in equivalent weight flow), while that for the 2-6 engines nearly parallels the surge line. Lowering the turbine-inlet temperature drives the outer compressors toward surge. Raising the turbine-inlet temperature drives the inner compressor of the 6-2 engines toward surge and that of the 2-6 engines toward a region of poor efficiency at high pressure ratio and weight flow.

8. The variation in engine power with turbine-inlet temperature is nearly linear; and, except for temperatures below 2000° R, the specific fuel consumption is nearly constant.

9. For operation with constant exhaust-nozzle area, the design stress, frontal area, and pressure ratio for the outer turbine increase considerably with flight speed and altitude. It appears desirable, therefore, to employ an adjustable exhaust-nozzle area that can be closed down as flight speed and altitude increase in order to eliminate these variations.

10. The design requirements of the inner turbine are not affected to any extent by the flight condition.

Comparison of two-spool engine characteristics with those of single-spool and free-turbine engines investigated previously revealed that

1. The variations of specific fuel consumption with turbine-inlet temperature for the two-spool engines are considerably less than for a single-spool engine of comparable compressor pressure ratio.

2. Increasing the pressure ratio obtained in the outer compressor of a two-spool engine results in characteristics similar to those of a single-spool engine, while reversing the split results in characteristics similar to those of a free-turbine engine.

3. Comparison of the two-spool and single-spool engines, for those aspects investigated herein, does not reveal any major limitations or differences which clearly indicate that one type is inherently better than the other.

Lewis Flight Propulsion Laboratory
National Advisory Committee for Aeronautics
Cleveland, Ohio, March 25, 1957

[redacted]

APPENDIX A

SYMBOLS

A	area, sq ft
a	velocity of sound based on local static temperature, ft/sec
c_p	specific heat at constant pressure, Btu/(lb)(^oR)
F	jet thrust, lb
f	fuel-air ratio
g	acceleration due to gravity, 32.17 sec^2
$\overline{H}$	lower heating value of fuel at 600^o R, Btu/lb
H/C	hydrogen-carbon ratio of fuel
h	enthalpy, Btu/lb
J	mechanical equivalent of heat, 778 ft-lb/Btu
P*	engine power (shaft horsepower plus equivalent shaft horsepower of net thrust), hp
p	pressure, lb/sq ft
R	gas constant, 53.3 ft-lb/(lb)(^oR)
r	radius from axis of rotation, ft
S	centrifugal stress, psi
sfc	specific fuel consumption (based on engine power P*), lb/hp-hr
T	temperature, ^oR
U	blade speed, ft/sec
V	velocity, ft/sec
W	velocity relative to rotor blades, ft/sec
w	weight flow, lb/sec

α absolute flow angle measured from axial direction (positive in direction of rotation), deg

Γ turbine blade-metal density, lb/cu ft

γ ratio of specific heats

δ ratio of pressure to NACA standard sea-level pressure of 2116 lb/sq ft

η efficiency

θ ratio of temperature to NACA standard sea-level temperature of 518.7° R

ρ density, lb/cu ft

φ stress-reduction factor for tapered blades

$\psi_h \equiv \{[h(\text{combustion products}) - h_a](1 + f)\}/f$ (see ref. 5), Btu/lb

ω angular rotative speed, radians/sec

Subscripts:

a air

an annular

B combustor

b blade

C compressor

cr conditions at Mach number of 1.0

d design

f fuel

g gearbox

h hub

j jet

m mean

p propeller

sl NACA standard sea-level conditions

T turbine

t tip

th throat

u tangential

x axial

0 ambient

1 outer-compressor inlet

2 inner-compressor inlet

3 combustor inlet

4 inner-turbine inlet

5 outer-turbine inlet

6 outer-turbine outlet

7 exhaust-nozzle outlet

Superscripts:

' total or stagnation state

" total or stagnation state relative to rotor

APPENDIX B

ANALYTICAL PROCEDURE

The assumptions made are given in the ANALYSIS section of this report. The following three flight conditions were investigated for a range of turbine-inlet temperature from 1600° to 2600° R:

Flight condition	Altitude, ft	Flight velocity, mph	Flight Mach number
X	0	0	0
Y	19,000	400	.564
Z	40,000	600	.906

Compressor Performance Maps

The compressor maps were constructed by use of the curves and method given in chapter X of reference 4. With this method it is necessary to select at the design point (100-percent equivalent design speed and design pressure ratio) a design value of weight flow per unit frontal area for the outer compressor and a design-point efficiency for both the inner and outer compressors. A small-stage efficiency of 0.90 was assigned for all compressors at the design point, and all outer compressors were assigned an equivalent weight flow per unit frontal area of 35 pounds per second per square foot at the design point. The performance maps obtained by this method are shown in figure 2.

Cycle Calculations

A series of figures (figs. 3 to 8) was constructed for each engine as described herein to investigate the variation in the parameters of interest with flight condition, turbine-inlet temperature, and inner-turbine pressure ratio p_4'/p_5'. A change in the inner-turbine pressure ratio p_4'/p_5' indicates an adjustment of the outer-turbine stators. Stator adjustment for the inner turbine was not considered in constructing the figures for reasons that will be discussed later. In constructing most of the figures the ratio of exhaust-nozzle area to outer-compressor frontal area $A_7/A_{t,1}$ was considered constant at 1.4 (i.e., the exhaust-nozzle area was considered fixed). The advantages of using a variable exhaust-nozzle area are discussed in the text.

The variations of p_2'/p_1', p_3'/p_2', p_4'/p_5', p_5'/p_6', $w\sqrt{\theta_1'}/\delta_1' A_{t,1}$, $w\sqrt{\theta_2'}/\delta_2' A_{t,1}$, $w\sqrt{\theta_5'}/\delta_5' A_{t,1}$, $P^*/A_{t,1}$, and sfc with turbine-inlet temperature T_4' for one flight condition (shown, e.g., in figs. 3 to 6) were obtained as follows:

Assign (1) Flight velocity V_0

(2) Altitude

(3) Turbine-inlet temperature T_4'

Assume (1) Rotative speed of outer compressors constant at design value ($\omega_1 = \omega_{1,d}$)

(2) Air weight flow through compressors equal to gas weight flow through turbines

(3) Equivalent weight flow into inner turbine $w\sqrt{\theta_4'}/\delta_4'$ constant

The value of the constant in assumption (3) is determined at the sea-level static condition with the compressors operating at their design point and the turbine-inlet temperature at 2100° R. The first stator in a conventional turbine operates at or near the choked condition in the turbine design operating range; and, therefore, $w\sqrt{\theta'}/\delta' A_{th}$ can be assumed with little error to be constant. Assuming, therefore, that $w\sqrt{\theta'}/\delta'$ is constant implies that the throat area of the first stator A_{th} is constant or, for the purposes of this report, that no stator adjustment is considered. The other assumptions used in the analysis are listed in table II. All parameters shown herein refer (except where noted by appropriate subscripts) to mean or mean-radius conditions at the stations considered.

Figure 3(a). - The percent equivalent design speed at which the outer compressor is operating is determined by the flight velocity and altitude, because

$$\% \text{ Equivalent design speed} = \frac{\omega_1\sqrt{\theta_1'}}{\omega_{1,d}} = \frac{1}{\sqrt{\theta_1'}} \tag{1}$$

and θ_1' is a function of only the flight velocity and altitude. Select from figure 2(e) a set of p_2'/p_1', $w\sqrt{\theta_1'}/\delta_1' A_{t,1}$, and $\eta_{C,1}$ lying on the percent-equivalent-design-speed line determined by the flight velocity and altitude assigned.

The continuity relation between stations 1 and 4 can be written as

$$\frac{w\sqrt{\theta_1'}}{\delta_1' A_{t,1}} = \frac{w\sqrt{\theta_4'}}{\delta_4' A_{t,1}} \frac{p_4'}{p_3'} \frac{p_3'}{p_2'} \frac{p_2'}{p_1'} \sqrt{\frac{T_1'}{T_4'}} \tag{2}$$

and, for the values already determined and an assigned value of T_4', it is possible to calculate the value of p_3'/p_2'. From the work relation

$$\frac{T_2'}{T_1'} - 1 = \frac{1}{\eta_{C,1}} \left[\left(\frac{p_2'}{p_1'} \right)^{\frac{\gamma_C - 1}{\gamma_C}} - 1 \right] \tag{3}$$

the temperature ratio T_2'/T_1' can also be calculated. This temperature ratio T_2'/T_1' and pressure ratio p_2'/p_1', with the continuity relation between stations 1 and 2,

$$\frac{w\sqrt{\theta_1'}}{\delta_1' A_{t,1}} = \frac{w\sqrt{\theta_2'}}{\delta_2' A_{t,1}} \frac{p_2'}{p_1'} \sqrt{\frac{T_1'}{T_2'}} \tag{4}$$

determine the value of the equivalent weight flow at the inlet of the inner compressor $w\sqrt{\theta_2'}/\delta_2' A_{t,1}$. With $w\sqrt{\theta_2'}/\delta_2' A_{t,1}$ and p_3'/p_2' known, read $\eta_{C,2}$ from the inner-compressor map (fig. 2(f)). The pressure ratio across the inner turbine p_4'/p_5' can then be calculated from the following work relation:

$$\frac{c_{p,C}}{\eta_{C,2}} T_2' \left[\left(\frac{p_3'}{p_2'} \right)^{\frac{\gamma_C - 1}{\gamma_C}} - 1 \right] = \eta_{T,4} c_{p,T} T_4' \left[1 - \left(\frac{p_5'}{p_4'} \right)^{\frac{\gamma_T - 1}{\gamma_T}} \right] \tag{5}$$

This procedure is repeated for other selected sets of $w\sqrt{\theta_1'}/\delta_1' A_{t,1}$, p_2'/p_1', and $\eta_{C,1}$ along the outer-compressor speed line determined by flight condition. Finally, T_4' is changed, and the procedure is again repeated. With the values calculated, plots of p_2'/p_1' against p_4'/p_5' for constant values of T_4', and p_3'/p_2' against p_4'/p_5' for constant values of T_4' can be made. Cross-plotting from these figures results in the type of figure shown in figure 3(a).

Figure 4(a). - Figure 4 is obtained much more simply than figure 3, from equations (3) and (4). For the sets of $w\sqrt{\theta_1'}/\delta_1' A_{t,1}$, p_2'/p_1', and $\eta_{C,1}$ selected along the outer-compressor speed line determined by the flight conditions, values of $w\sqrt{\theta_2'}/\delta_2' A_{t,1}$ can be calculated from equations (3) and (4). These values are then plotted as shown in figure 4(a).

Figure 5(a). - For each T_4' and set of p_2'/p_1', $w\sqrt{\theta_1'}/\delta_1' A_{t,1}$, and $\eta_{C,1}$, assign a range of p_5'/p_6' consistent with the limits imposed by the following two requirements: (1) that the outer turbine produce at least as much work as the outer compressor, and (2) that the ratio of exhaust-nozzle area to outer-compressor frontal area $A_7/A_{t,1}$ be finite. Calculate T_5' from the work relation,

$$1 - \frac{T_5'}{T_4'} = \eta_{T,4}\left[1 - \left(\frac{p_5'}{p_4'}\right)^{\frac{\gamma_T - 1}{\gamma_T}}\right] \tag{6}$$

Then calculate the specific work or specific enthalpy changes $\Delta h_{5-6}'$ and $\Delta h_{1-2}'$ as follows:

$$\Delta h_{5-6}' = \eta_{T,5} c_{p,T} T_5' \left[1 - \left(\frac{p_6'}{p_5'}\right)^{\frac{\gamma_T - 1}{\gamma_T}}\right], \text{ Btu/lb} \tag{7}$$

$$\Delta h_{1-2}' = \frac{c_{p,C} T_1'}{\eta_{C,1}} \left[\left(\frac{p_2'}{p_1'}\right)^{\frac{\gamma_C - 1}{\gamma_C}} - 1\right], \text{ Btu/lb} \tag{8}$$

The pressure ratio left to produce jet thrust is

$$\frac{p_7'}{p_0} = \frac{p_7'}{p_6'}\frac{p_6'}{p_5'}\frac{p_5'}{p_4'}\frac{p_4'}{p_3'}\frac{p_3'}{p_2'}\frac{p_2'}{p_1'}\frac{p_1'}{p_0'}\frac{p_0'}{p_0} \tag{9}$$

where the pressure ratios on the right side of equation (9) have all been assumed or calculated. The jet velocity is calculated from the isentropic relation

$$\frac{T_j}{T_7'} = \left(\frac{p_0}{p_7'}\right)^{\frac{\gamma_T - 1}{\gamma_T}} \tag{10}$$

and the energy relation

$$\frac{T_j}{T'_7} = \left[1 - \frac{\gamma_T - 1}{\gamma_T + 1}\left(\frac{V_j}{a'_{cr,7}}\right)^2\right] \tag{11}$$

where

$$T'_7 = T'_6, \ ^\circ R$$

and

$$a'_{cr,7} = \sqrt{\frac{2\gamma_T}{\gamma_T + 1} gRT'_7}, \ ft/sec \tag{12}$$

The thrust per unit outer-compressor frontal area is then

$$\frac{F}{A_{t,1}} = \frac{w}{A_{t,1}} \frac{V_j - V_0}{g}, \ lb/sq \ ft \tag{13}$$

where

$$\frac{w}{A_{t,1}} = \frac{w\sqrt{\theta'_1}}{\delta'_1 A_{t,1}} \frac{\delta'_1}{\sqrt{\theta'_1}}, \ (lb/sec)/sq \ ft \tag{14}$$

The engine power in terms of equivalent shaft power is obtained from the following equation:

$$\frac{P^*}{A_{t,1}} = \frac{J\eta_g}{550} \frac{w}{A_{t,1}} (\Delta h'_{5-6} - \Delta h'_{1-2}) + V_0 \left(\frac{F}{A_{t,1}}\right) \frac{1}{550\eta_p}, \ hp/sq \ ft \tag{15}$$

For the case when there is no forward velocity V_0 (sea-level static condition), a conversion factor of 3.62 pounds of thrust for shaft horsepower is assumed to convert static thrust to equivalent shaft horsepower. For the sea-level static condition, therefore,

$$\frac{P^*}{A_{t,1}} = \frac{J\eta_g}{550} \frac{w}{A_{t,1}} (\Delta h'_{5-6} - \Delta h'_{1-2}) + \frac{F}{A_{t,1}} \frac{1}{3.62}, \ hp/sq \ ft \tag{16}$$

In calculating the exhaust-nozzle area A_7, two conditions are recognized. For the choked-exhaust-nozzle conditions, when

$$\frac{p_7'}{p_0} \geq \left(\frac{\gamma_T + 1}{2}\right)^{\frac{\gamma_T}{\gamma_T - 1}} = 1.8324 \tag{17}$$

then

$$\left(\frac{\rho V}{\rho' a_{cr}'}\right)_7 = \left(\frac{2}{\gamma_T + 1}\right)^{\frac{1}{\gamma_T - 1}} = 0.6276 \tag{18}$$

and the ratio of exhaust-nozzle area to outer-compressor frontal area $A_7/A_{t,1}$ is calculated from the following continuity relation:

$$\frac{A_7}{A_{t,1}} \left(\frac{\rho V}{\rho' a_{cr}'}\right)_7 \frac{p_7'}{RT_7'} \sqrt{\frac{2\gamma_T}{\gamma_T + 1} gRT_7'} = \frac{w}{A_{t,1}} \tag{19}$$

For the unchoked condition, when

$$\frac{p_7'}{p_0} < \left(\frac{\gamma_T + 1}{2}\right)^{\frac{\gamma_T}{\gamma_T - 1}} \tag{20}$$

it is assumed that $p_0 = p_7$ and, therefore,

$$\left(\frac{\rho V}{\rho' a_{cr}'}\right)_7 = \left(\frac{p_0}{p_7'}\right)^{\frac{1}{\gamma_T}} \sqrt{\left[1 - \left(\frac{p_0}{p_7'}\right)^{\frac{\gamma_T - 1}{\gamma_T}}\right] \frac{\gamma_T + 1}{\gamma_T - 1}} \tag{21}$$

The value of $(\rho V/\rho' a_{cr}')_7$ obtained from equation (21) is then introduced into equation (19) to obtain the area ratio $A_7/A_{t,1}$ for the unchoked condition.

The fuel-air ratio f is calculated using reference 6, where

$$f = \frac{h_{a,4} - h_{a,3}}{\eta_B \overline{H} - h_{a,4} - \psi_{h,4} + h_f}, \text{ lb fuel/lb air} \tag{22}$$

and

$$\overline{H} = 15{,}935 + 15{,}800(H/C) \tag{23}$$

With the combustor-inlet and -outlet temperatures known and the values of H/C, η_B, and h_f assigned, the fuel-air ratio is calculated using charts I and IV of reference 6.

The specific fuel consumption sfc is then obtained from the following equation:

$$\text{sfc} = \frac{f\left(\frac{w}{A_{t,1}}\right)3600}{\frac{P^*}{A_{t,1}}}, \text{ lb/hp-hr} \tag{24}$$

This procedure is repeated selecting other sets of $w\sqrt{\theta_1'}/\delta_1' A_{t,1}$, p_2'/p_1', and $\eta_{C,1}$ along the outer-compressor speed line determined by the flight condition. Finally, T_4' is changed and the procedure is again repeated. For each turbine-inlet temperature, plots are made of $P^*/A_{t,1}$ against $A_7/A_{t,1}$ and sfc against $A_7/A_{t,1}$ for the values of p_2'/p_1' selected. From these plots and figure 3(a), cross plots at a constant area ratio $A_7/A_{t,1}$ of 1.4 are made as shown in figure 5(a).

Figure 6(a). - For the assigned values of p_5'/p_6', p_2'/p_1', T_4', and calculated values of $A_7/A_{t,1}$, a plot of p_5'/p_6' against $A_7/A_{t,1}$ for constant values of p_2'/p_1' can be made for each T_4'. From these figures and figure 3(a), cross plots at a constant area ratio $A_7/A_{t,1}$ of 1.4 are made as shown in figure 6(a).

The straight vertical lines in figure 6(a) denoting constant values of equivalent weight flow at the outer-turbine inlet are obtained using the following continuity relation:

$$\frac{w\sqrt{\theta_4'}}{\delta_4' A_{t,1}} = \frac{w\sqrt{\theta_5'}}{\delta_5' A_{t,1}} \frac{p_5'}{p_4'} \sqrt{\frac{T_4'}{T_5'}} \tag{25}$$

Since $w\sqrt{\theta_4'}/\delta_4' A_{t,1}$ and $\eta_{C,4}$ are constant, only one value of $w\sqrt{\theta_5'}/\delta_5' A_{t,1}$ occurs for each p_4'/p_5', and hence the straight vertical lines shown in figure 6(a).

Other considerations. - It was pointed out in reference 3 that for single-spool engines an area ratio $A_7/A_{t,1}$ of 1.4 resulted in nearly maximum power and minimum sfc at all flight conditions over the range of turbine-inlet temperature of interest. This was also found to be the case for the two-spool engine when the figures used to cross-plot figure 5 were examined. In order to eliminate one of the variables, therefore, the calculated values were cross-plotted to obtain the figures as shown for a constant area ratio $A_7/A_{t,1}$ of 1.4. It was also found that much the same variation shown in figure 5 of $P^*/A_{t,1}$ and sfc with p_4'/p_5' occurred over a range of $A_7/A_{t,1}$.

4301

The parameters are plotted against p_4'/p_5' in order to determine whether it might be desirable to incorporate turbine stator adjustment in the outer turbine. From equation (25) it can be seen that, if $w\sqrt{\theta_4'}/\delta_4' A_{t,1}$ and $w\sqrt{\theta_5'}/\delta_5' A_{t,1}$ are constant (i.e., no turbine stator adjustment in either turbine), then p_4'/p_5' will be constant. The case of no stator adjustment (p_4'/p_5' = const.) can thus be easily compared in the figures presented with the case of stator adjustment in the outer turbine.

The case of stator adjustment for both the inner and outer turbines ($w\sqrt{\theta_4'}/\delta_4' A_{t,1}$ and $w\sqrt{\theta_5'}/\delta_5' A_{t,1}$ allowed to vary) was considered, but the results are not presented. In this part of the analysis the procedure was to assign various values of p_2'/p_1' along the speed line determined by the flight condition and operation at constant outer-compressor rotative speed and then vary p_3'/p_2' over the maximum range possible consistent with the inner-compressor map characteristics. For each p_2'/p_1', p_3'/p_2', and T_4', a total-energy term representing the energy available for either propeller or jet thrust was calculated. An sfc based on this total energy was also calculated. Plots were made for each T_4' and flight condition of sfc against p_3'/p_2' for various p_2'/p_1'. From these plots the compressor operating conditions for minimum sfc for a given turbine-inlet temperature and flight condition were determined. Comparison of these minimums with those obtained for the compressor operating conditions with turbine stator adjustment of only the outer-turbine stators showed that the improvements made available by adjusting both turbines stators were small in most instances and did not warrant the added engine complexity required to obtain the improvements.

Turbine Stress, Component Frontal Areas, and

Compressor Design Specifications

The design problems and features of any one engine component cannot be isolated from the design problems and features of the other components. For example, the compressor aerodynamics will be compromised by the turbine stress limitations. In this section, the construction of figures used to investigate some of these compromises and some of the geometric features of the engine are explained.

Outer spool. - The stresses of concern in this report are the centrifugal stresses at the hub of the last rotor of both the inner and outer turbines. Reference 7 develops the following equation for the centrifugal stress at the hub of a rotor blade:

$$S_b = \frac{\rho_b \omega^2 A_{an}}{2\pi g} \frac{\varphi}{144}, \text{ psi} \tag{26}$$

Then, the equation for the hub stress of the last rotor of the outer turbine can be written as

$$S_{b,6} = \frac{\rho_b U_{t,1}^2}{2g} \frac{A_{an,6}}{A_7} \frac{A_7}{A_{t,1}} \frac{\varphi}{144} \tag{27}$$

or, applying continuity between stations 6 and 7, as

$$S_{b,6} = \frac{\rho_b U_{t,1}^2}{2g} \frac{p_7'}{p_6'} \frac{\left(\frac{\rho V}{\rho' a_{cr}'}\right)_7}{\left(\frac{\rho V}{\rho' a_{cr}'}\right)_6} \frac{A_7}{A_{t,1}} \frac{\varphi}{144} \tag{28}$$

In calculating stress values, the turbines were assumed to be designed up to the limiting-loading point, or with $(\rho V/\rho' a_{cr}')_6$ a maximum. For most turbines, limiting loading occurs at about an exit axial Mach number of 0.7 (ref. 8), or a value of 0.5725 for $(\rho V/\rho' a_{cr}')_6$ when the exit tangential component of velocity is zero. The stress for a turbine designed at limiting loading will thus be at a minimum for a given exit gas total state and weight flow, since $(\rho V/\rho' a_{cr}')_6$ is a maximum (see eq. (28)). Changing the gas exit total state by varying the area ratio $A_7/A_{t,1}$ and its attendant effects on turbine stress and frontal area are discussed in the text.

[redacted]

It is seen from equation (28) that the stress $S_{b,6}$ is a function of only the specific weight flow at station 7 if

(1) All turbines are designed at limiting loading (i.e., $(\rho V/\rho' a'_{cr})_6 = \text{const.}$).

(2) The outer-compressor rotative speed is constant (and, consequently, $U_{t,1}$ is constant).

(3) The area ratio $A_7/A_{t,1}$ is constant.

(4) The assumptions of table II are applied.

Thus,

$$S_{b,6} = \text{const.} \left(\frac{\rho V}{\rho' a'_{cr}}\right)_7 \tag{29}$$

In order to determine the value of the constant in equation (29) it is necessary to assign a blade tip speed $U_{t,1}$. The design blade tip speed assigned was 1124 feet per second. This blade tip speed, with the value of equivalent weight flow per unit frontal area of 35 pounds per second per square foot assigned in constructing the compressor performance maps, results for a 0.4 hub-tip radius ratio in an inlet axial Mach number of 0.6 and an inlet relative Mach number at the tip of the rotor of 1.2. The first stage of the outer compressor being considered, then, is an advanced transonic stage. Therefore, the resulting turbine stresses are rather high, as will be seen from the stress figures to be presented.

From the continuity equation, it can be shown that the ratio of the outer-turbine to the outer-compressor frontal area $A_{t,6}/A_{t,1}$ can be written as

$$\frac{A_{t,6}}{A_{t,1}} = \frac{A_7}{A_{t,1}} \frac{p'_7}{p'_6} \frac{\left(\frac{\rho V}{\rho' a'_{cr}}\right)_7}{\left(\frac{\rho V}{\rho' a'_{cr}}\right)_6} \frac{1}{\left[1 - \left(\frac{r_h}{r_t}\right)^2_6\right]} \tag{30}$$

In the results presented herein it is assumed that the exit hub-tip radius ratio of all the outer turbines $(r_h/r_t)_6$ is 0.6. This is considered a practical lower limit, which, as can be seen from equation (30), would result in the minimum turbine frontal area $A_{t,6}$. (The

value of $(\rho V/\rho' a'_{cr})_6$ was assumed to be at its maximum value previously in order to minimize the stress $S_{b,6}$.) It can also be seen from equation (30) that the area ratio $A_{t,6}/A_{t,1}$, like the stress $S_{b,6}$, is a function of only the specific weight flow at the exhaust-nozzle exit; that is,

$$\frac{A_{t,6}}{A_{t,1}} = \text{const.} \left(\frac{\rho V}{\rho' a'_{cr}}\right)_7 \tag{31}$$

In calculating the area ratio $A_7/A_{t,1}$ (eqs. (17) to (21)), it was necessary to calculate the specific weight flow at station 7; and, therefore, it was possible to calculate the stress $S_{b,6}$ and the area ratio $A_{t,6}/A_{t,1}$. These calculated values were cross-plotted to obtain the type of figure shown in figure 7(a), which is a plot of $S_{b,6}$ and $A_{t,6}/A_{t,1}$ against inner-turbine pressure ratio p'_4/p'_5 for various turbine-inlet temperatures T'_4. The figure presents values for one flight condition, one compressor-pressure-ratio split, and one value of area ratio $A_7/A_{t,1}$ (1.4).

Inner spool. - The continuity equation (between stations 5 and 7), suitably modified to account for the pressure and temperature drops across the outer turbine, can be introduced into the stress relation given by equation (26) to give the following equation for the stress at station 5:

$$S_{b,5} = \frac{p'_7}{p'_6} \frac{\left(\frac{\rho V}{\rho' a'_{cr}}\right)_7}{\left(\frac{\rho V}{\rho' a'_{cr}}\right)_5} \frac{A_7}{A_{t,1}} \frac{A_{t,1}}{A_{t,2}} \frac{\rho_b U^2_{t,2}}{2g} \frac{\frac{p'_6}{p'_5}}{\sqrt{1 - \eta_{T,5}\left[1 - \left(\frac{p'_6}{p'_5}\right)^{\frac{\gamma_T - 1}{\gamma_T}}\right]}} \frac{\varphi}{144} \tag{32}$$

The equation for the ratio of inner-turbine to outer-compressor frontal area $A_{t,5}/A_{t,1}$ is obtained from the continuity equation

(between stations 5 and 7) suitably modified to account for the pressure and temperature drops across the outer turbine. One form of the area-ratio equation is as follows:

$$\frac{A_{t,5}}{A_{t,1}} = \frac{p'_7}{p'_6} \frac{\left(\frac{\rho V}{\rho' a'_{cr}}\right)_7}{\left(\frac{\rho V}{\rho' a'_{cr}}\right)_5} \frac{A_7}{A_{t,1}} \frac{1}{\left[1 - \left(\frac{r_h}{r_t}\right)_5^2\right]} \frac{\frac{p'_6}{p'_5}}{\sqrt{1 - \eta_{T,5}\left[1 - \left(\frac{p'_6}{p'_5}\right)^{\frac{\gamma_T - 1}{\gamma_T}}\right]}} \tag{33}$$

It can be seen from equation (33) that, if all inner turbines are specified to have exit hub-tip radius ratios $(r_h/r_t)_5$ of 0.6 and to be designed at limiting loading ($(\rho V/\rho' a'_{cr})_5 = 0.5725$), the area ratio $A_{t,5}/A_{t,1}$ can be calculated from previously obtained values. As noted previously, the stress is minimized when the exit specific-mass-flow term is a maximum. When, in addition, the exit hub-tip radius ratio is minimized, the minimum turbine frontal area is also obtained.

Examination of stress equation (32) shows that it is necessary to specify an area ratio $A_{t,1}/A_{t,2}$ and some design tip speed for the inner compressor in order to calculate values for the stress $S_{b,5}$. The procedure for doing this will be outlined. Selection of the design values of $U_{t,2}$ and $A_{t,1}/A_{t,2}$ involved a compromise between the compressor aerodynamic and size requirements and the inner-turbine stress. Since the stress $S_{b,5}$ was not expected to vary greatly with either turbine-inlet temperature or flight condition, the problem of selecting design values of $U_{t,2}$ and $A_{t,1}/A_{t,2}$ was investigated at the sea-level static condition with the turbine-inlet temperature at 2100° R, the compressors operating at their respective design points, and a ratio of exhaust-nozzle to outer-compressor frontal area of 1.4. With these stipulations, equation (32) could be written (multiplying the right side of the equation by θ'_2/θ'_2) as

$$S_{b,5} = \text{const.} \left(\frac{U_t}{\sqrt{\theta'}}\right)_2^2 \frac{A_{t,1}}{A_{t,2}} \tag{34}$$

where the constant is different for each compressor-pressure-ratio split. The parameter $(U_t/\sqrt{\theta'})_2^2 (A_{t,1}/A_{t,2})$ is, then, a parameter relating turbine stress to the aerodynamics and size of the compressor

and therefore was one of the parameters investigated. The constant in equation (34) has a value of 0.01430, 0.01685, and 0.01800 for the 6-2, 3-4, and 2-6 compressor-pressure-ratio splits, respectively.

Three sets of figures were devised for each compressor-pressure-ratio split to investigate the effect on the stress parameter $(U_t/\sqrt{\theta'})_2^2 \times (A_{t,1}/A_{t,2})$ of variations in, for example, the relative tip Mach number and frontal area at the inlet of the inner compressor. The following equations were used to construct a set of these figures (figs. 9(a) to (c), e.g.):

(1) The velocity-diagram relations:

$$\left(\frac{V_u}{a'_{cr}}\right)_{2,t} = \left(\frac{V_x}{a'_{cr}}\right)_{2,t} \tan \alpha_{2,t} \tag{35}$$

$$\left(\frac{W}{a}\right)_{2,t} = \frac{\sqrt{\frac{2}{\gamma_c + 1}}\left(\frac{W}{a'_{cr}}\right)_{2,t}}{\sqrt{1 - \frac{\gamma_c - 1}{\gamma_c + 1}\left[\left(\frac{V_x}{a'_{cr}}\right)_{2,t}^2 + \left(\frac{V_u}{a'_{cr}}\right)_{2,t}^2\right]}} \tag{36}$$

$$\left(\frac{W}{a'_{cr}}\right)_{2,t}^2 = \left(\frac{V_x}{a'_{cr}}\right)_{2,t}^2 + \left(\frac{U - V_u}{a'_{cr}}\right)_{2,t}^2 \tag{37}$$

(2) The expression for equivalent speed in terms of (U/a'_{cr}):

$$\left(\frac{U}{\sqrt{\theta'}}\right)_{2,t} = \left(\frac{U}{a'_{cr}}\right)_{2,t} \sqrt{\frac{2\gamma_c}{\gamma_c + 1} gRT_{sl}} \tag{38}$$

(3) The free-vortex and simple-radial-equilibrium relation for V_u and specific weight flow:

$$\left(\frac{V_u}{a'_{cr}}\right)_{2,m} = \left(\frac{V_u}{a'_{cr}}\right)_{2,t} \frac{2}{\left[1 + \left(\frac{r_h}{r_t}\right)_2\right]} \tag{39}$$

$$\left(\frac{\rho V_x}{\rho' a'_{cr}}\right)_{2,m} = \left(\frac{V_x}{a'_{cr}}\right)_{2,t}\left\{1 - \frac{\gamma_c - 1}{\gamma_c + 1}\left[\left(\frac{V_x}{a'_{cr}}\right)^2_{2,t} + \left(\frac{V_u}{a'_{cr}}\right)^2_{2,m}\right]\right\}^{\frac{1}{\gamma_c - 1}} \quad (40)$$

That is, (V_x/a'_{cr}) is considered constant over the blade height.

(4) The continuity relation:

$$\frac{w\sqrt{\theta'_2}}{\delta'_2 A_{an,2}} = \frac{w\sqrt{\theta'_1}}{\delta'_1 A_{t,1}}\sqrt{\frac{T'_2}{T'_1}}\frac{p'_1}{p'_2}\frac{A_{t,1}}{A_{t,2}}\frac{1}{\left[1 - \left(\frac{r_h}{r_t}\right)^2_2\right]} \quad (41)$$

where $(\rho V_x/\rho' a'_{cr})_{2,m}$ is considered the average specific weight flow; and, therefore,

$$\frac{w\sqrt{\theta'_2}}{\delta'_2 A_{an,2}} = \frac{p_{sl}}{\sqrt{T_{sl}}}\sqrt{\frac{2\gamma_c}{\gamma_c + 1}\frac{g}{R}}\left(\frac{\rho V_x}{\rho' a'_{cr}}\right)_{2,m} \quad (42)$$

An axial velocity distribution from stations 1 to 3 that would result in good compressor staging characteristics and good combustor-inlet conditions was also specified in order to select a reasonable value of $(V_x/a'_{cr})_2$ for the different compressor-pressure-ratio splits. This distribution of axial velocity is shown in figure 9(d) as a plot of axial velocity against compressor pressure ratio. The pressure ratio from 1 to 12 is plotted on the logarithmic scale of the abscissa in order to simulate a plot of axial velocity against stage number. Advanced compressor designs indicate that a constant axial velocity across the first few stages followed by a linear reduction to the axial velocity at the exit of the compressor results in acceptable stage velocity diagrams and rates of diffusion. The inlet velocity at station 1 for the conditions previously specified was 648 feet per second, and an exit velocity of 400 feet per second was assigned at station 3. An exit velocity of 400 feet per second is quite acceptable as a combustor-inlet velocity and, as will be seen, permits a wide choice of frontal area and hub-tip radius ratio at the exit of the inner compressor (station 3). An exit velocity of 400 feet per second also results in only a moderate reduction in velocity from the inlet velocity of 648 feet per second and should, therefore, result in low stage diffusion rates. With the axial velocity distribution shown in figure 9(d), then, the values obtained for $(V_x/a'_{cr})_2$ were 0.3658, 0.4873, and 0.5692 for the 6-2, 3-4, and 2-6 compressor-pressure-ratio splits, respectively.

Shown in figure 9(e) are the variations in outlet axial velocity ratio $(V_x/a'_{cr})_3$ with the compressor-outlet geometry parameters $A_{t,3}/A_{t,1}$ and $(r_h/r_t)_3$. This figure is the same for all compressor-pressure-ratio splits, since the same small-stage compressor efficiency was assumed at the compressor design points. This figure was constructed using the continuity relation between stations 1 and 3, the equivalent weight flow and hub-tip radius ratio at station 1 being the same for all compressor-pressure-ratio splits. The exit velocity of 400 feet per second selected in figure 9(d) results in $(V_x/a'_{cr})_3$ of 0.2643. From figure 9(e) it can be seen that this value of $(V_x/a'_{cr})_3$ permits a wide selection of $(r_h/r_t)_3$ and $A_{t,3}/A_{t,1}$.

4301

The last figure used in selecting the design blade tip speeds and frontal areas for the inner compressors is figure 9(f), which determines the allowable stress for the inner turbine. The allowable stress is a function of the material used in the turbine rotor blade and the temperature of this material. The blade-metal temperature is a function of the blade stress, as can be seen by introducing the stress equation into the energy equation:

$$T''_{5,h} = T'_5 + \frac{U^2_{5,h}}{2gJc_{p,T}} \tag{43}$$

where $V_{u,5} = 0$. The result of this substitution gives the following expression:

$$T''_{5,h} = T'_5 + \frac{\left(\frac{r_h}{r_t}\right)^2_5 (S_{b,5}) \quad (144)}{Jc_{p,T}\rho_b\varphi\left[1 - \left(\frac{r_h}{r_t}\right)^2_5\right]} \tag{44}$$

which, if the relative total temperature $T''_{5,h}$ is assumed the same as the blade-metal temperature, shows that the blade-metal temperature is a linear function of the blade stress for a given T'_5. The values of T'_5 for the three compressor-pressure-ratio splits were calculated for a turbine-inlet temperature T'_4 of 2100° R and introduced into equation (44) to obtain the straight-line relations shown in figure 9(f) for the three compressor-pressure-ratio splits. Also shown in figure 9(f) is the experimental 1000-hour stress-rupture curve for a common high-temperature material (HS-31, ref. 9). The intersection of the stress-rupture curve with the individual straight-line relation of the

three compressor-pressure-ratio splits determines the allowable stresses for a 1000-hour life. Stresses below these intersections will result in longer life or permit higher temperatures with a 1000-hour life.

The procedure for selecting the design equivalent tip speed and frontal area for each compressor-pressure-ratio split is as follows: Select an allowable turbine stress from figure 9(f) and the axial velocity into the inner compressor from figure 9(d). With $V_{x,2}$ selected, calculate the velocity ratio $(V_x/a'_{cr})_2$. Using the allowable stress, calculate the allowable $(U_t/\sqrt{\theta'})_2^2 (A_{t,1}/A_{t,2})$ from equation (34). From figures 9(a), (b), (c), and (e) select the other compressor parameters of $(U_t/\sqrt{\theta'})_2$, $A_{t,2}/A_{t,1}$, α_2, $A_{t,3}/A_{t,1}$, $(r_h/r_t)_3$, and $(r_h/r_t)_2$ representing the best compromise of these parameters in regard to compressor geometry, aerodynamics, and minimum number of stages (high $(U_t/\sqrt{\theta'})_2$). The selections made for the three compressor-pressure-ratio splits along with the values assigned to the outer compressors are listed in table I. In selecting the values shown in table I, the inlet relative angle to the first rotor of the inner compressor was not allowed to exceed 65°. The allowable turbine stresses are also specified so that they are well within a 1000-hour life for the inlet temperature of 2100° R at the design point.

With the area ratio $A_{t,2}/A_{t,1}$ and $(U_t/\sqrt{\theta'})_{2,d}$ selected in this manner, the stresses at the other flight conditions and turbine-inlet temperatures can be calculated. These stresses and the area ratios $A_{t,5}/A_{t,1}$ (obtained in the manner described previously) are plotted against turbine pressure ratio p'_4/p'_5 for the various turbine-inlet temperatures T'_4 and one flight condition as shown in figure 8(a). Additional stipulations in plotting figure 8(a) are that the area ratio $A_7/A_{t,1}$ is constant at a value of 1.4 and that the inner turbine is without stator adjustment.

REFERENCES

1. Davison, Elmer H.: Turbine Design Considerations for Turbine-Propeller Engine Operating over a Range of Flight Conditions. NACA RM E53D16, 1953.

2. Davison, Elmer H.: Turboprop-Engine Design Considerations. I - Effect of Mode of Engine Operation on Performance of Turboprop Engine with Current Compressor Pressure Ratio. NACA RM E54D19, 1955.

4301

3. Davison, Elmer H., and Stalla, Margaret C.: Turboprop-Engine Design Considerations. II - Design Requirements and Performance of Turboprop Engines with a Single-Spool High-Pressure-Ratio Compressor. NACA RM E55B18, 1955.

4. Members of the Compressor and Turbine Research Division: Aerodynamic Design of Axial-Flow Compressors. Vol. II. NACA RM E56B03a, 1956.

5. Anon.: Technical Data on Allegheny Ludlum Alloy A-286. Allegheny Ludlum Steel Corp., 1952.

6. English, Robert E., and Wachtl, William W.: Charts of Thermodynamic Properties of Air and Combustion Products from 300° to 3500° R. NACA TN 2071, 1950.

7. LaValle, Vincent L., and Huppert, Merle C.: Effects of Several Design Variables on Turbine-Wheel Weight. NACA TN 1814, 1949.

8. English, Robert E., Silvern, David H., and Davison, Elmer H.: Investigation of Turbines Suitable for Use in a Turbojet Engine with High Compressor Pressure Ratio and Low Compressor-Tip Speed. I - Turbine-Design Requirements for Several Engine Operating Conditions. NACA RM E52A16, 1952.

9. Anon.: Haynes Alloys for High-Temperature Service. Haynes Stellite Co., c. 1949-1950.

4301

TABLE I. - COMPRESSOR DESIGN SPECIFICATIONS

[Sea-level static conditions and 2100° R turbine-inlet temp.]

	Engines (pressure-ratio split)		
	6-2	3-4	2-6
Equivalent tip speed, $(U_t/\sqrt{\theta'})_2$, ft/sec	1124	1124	1124
Hub-tip radius ratio, $(r_h/r_t)_1$	0.4	0.4	0.4
Equivalent weight flow per unit frontal area, $(w\sqrt{\theta'}/\delta' A_t)_1$, (lb/sec)/sq ft	35	35	35
Relative tip Mach number, $(W/a)_{t,1}$	1.2	1.2	1.2
Axial Mach number, $(V_x/a)_1$	0.6	0.6	0.6
Equivalent tip speed, $(U_t/\sqrt{\theta'})_2$, ft/sec	900	1110	1170
Hub-tip radius ratio, $(r_h/r_t)_2$	0.80	0.73	0.65
Relative tip Mach number, $(W/a)_{t,2}$	0.8	1.0	1.2
Ratio of frontal areas, $A_{t,2}/A_{t,1}$	0.78	0.88	0.86
Absolute flow angle, α_2, deg	15	15	0
Critical axial velocity ratio, $(V_x/a'_{cr})_2$	0.366	0.487	0.569
Hub-tip radius ratio, $(r_h/r_t)_3$	0.83	0.84	0.83
Ratio of frontal areas, $A_{t,3}/A_{t,1}$	0.70	0.73	0.70
Critical axial velocity ratio, $(V_x/a'_{cr})_3$	0.264	0.264	0.264
Allowable stress, $S_{b,5}$, psi	15,000	23,500	28,500

TABLE II. - ASSUMPTIONS

Inlet diffuser pressure ratio, p_1'/p_0'	1.00
Combustor pressure ratio, p_4'/p_3'	0.95
Exhaust-nozzle pressure ratio, p_7'/p_6'	0.95
Turbine efficiency (based on total-pressure ratio), η_T	0.85
Gearbox power-transmission efficiency, η_g	0.95
Propeller efficiency, η_p	0.80
Combustion efficiency, η_B	1.00
Hydrogen-carbon ratio of fuel, H/C	0.175
Initial enthalpy of fuel, h_f, Btu/lb	-50.0
Mechanical equivalent of heat, J, ft-lb/Btu	778.2
Gas constant, R, ft-lb/(lb)($^\circ$R)	53.3
Gravitational constant, g, ft/sec^2	32.17
Ratio of specific heats in compressor, γ_C	1.40
Ratio of specific heats in turbine, γ_T	1.30
Constant of conversion from static thrust to equivalent shaft power	3.62
Hub-tip radius ratio at inner-turbine outlet, $(r_h/r_t)_5$	0.60
Hub-tip radius ratio at outer-turbine outlet, $(r_h/r_t)_6$	0.60
Specific weight flow at inner-turbine outlet, $(\rho V/\rho' a_{cr}')_5$	0.5725
Specific weight flow at outer-turbine outlet, $(\rho V/\rho' a_{cr}')_6$	0.5725
Centrifugal-stress-reduction factor for tapered blades, φ	0.70
Turbine blade-metal density, Γ, lb/cu ft	500
Exit tangential components of velocity, $(V_{u,3}, V_{u,5}, V_{u,6})$	0

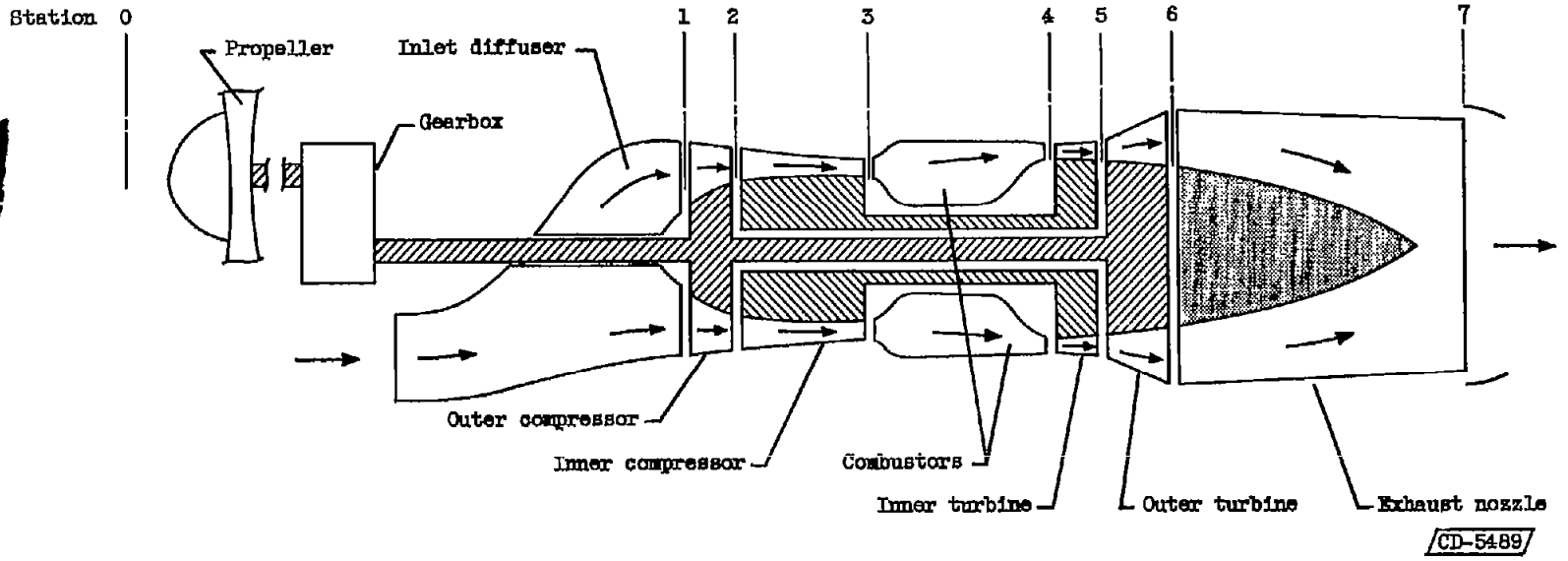

Figure 1. - Schematic diagram of two-spool turboprop engine.

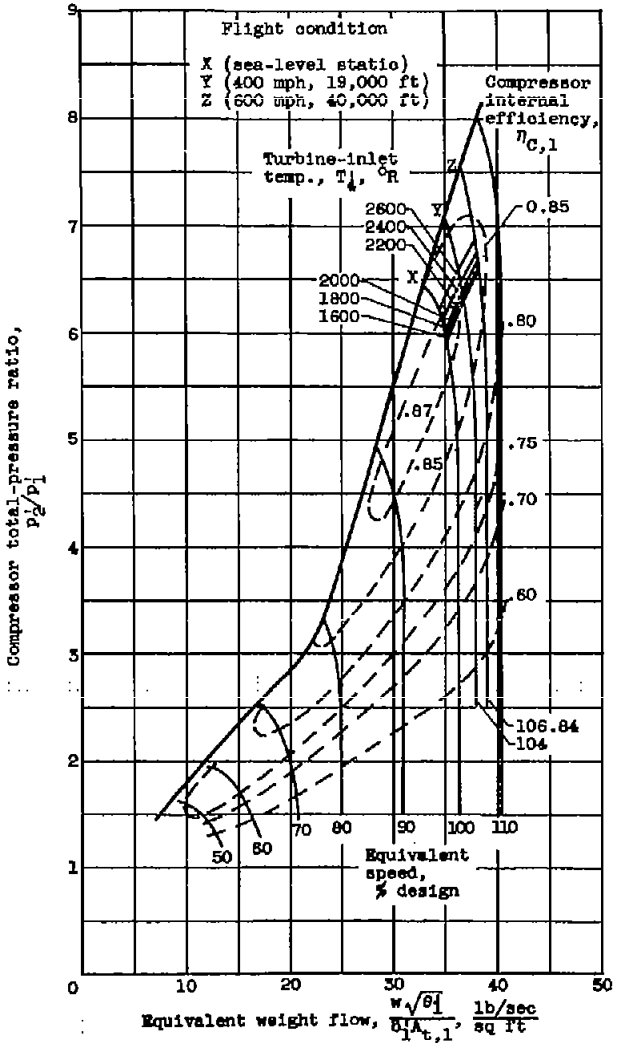

(a) Compressor-pressure-ratio split, 6-2; outer compressor.

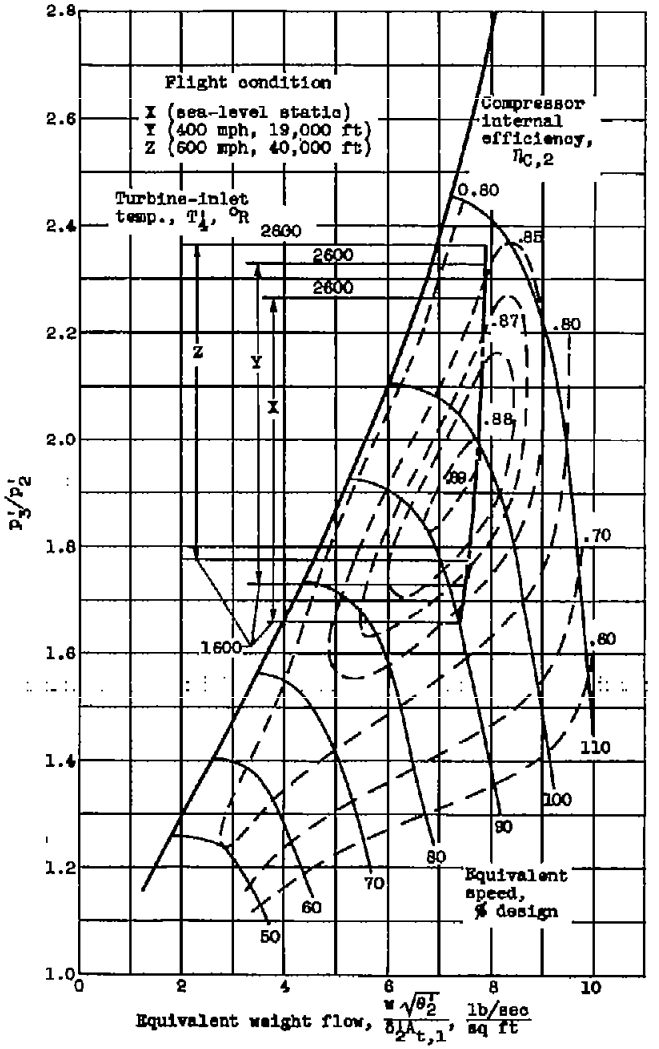

(b) Compressor-pressure-ratio split, 6-2; inner compressor.

Figure 2. - Compressor performance maps.

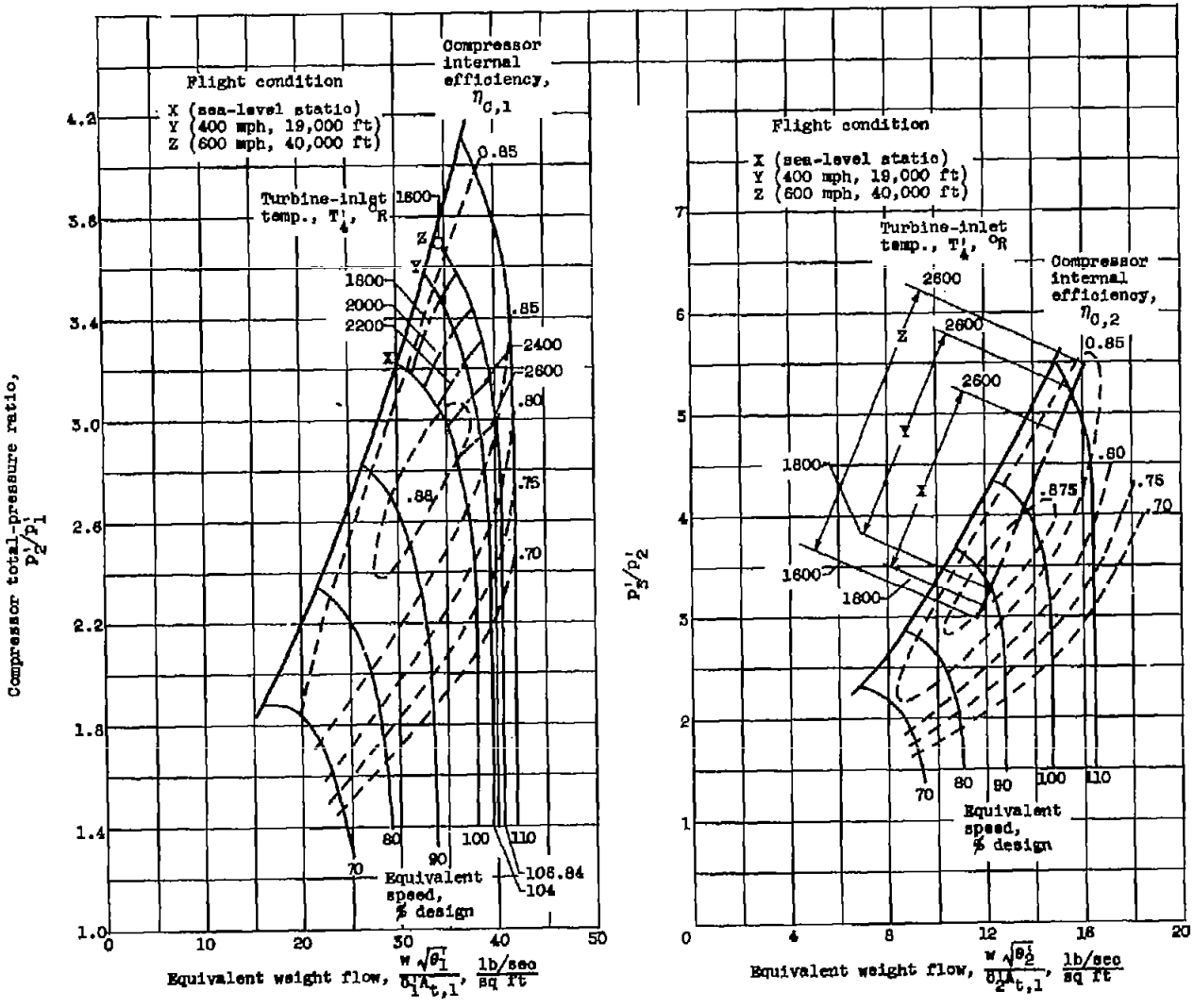

(c) Compressor-pressure-ratio split, 3-4; outer compressor.

(d) Compressor-pressure-ratio split, 3-4; inner compressor.

Figure 2. - Continued. Compressor performance maps.

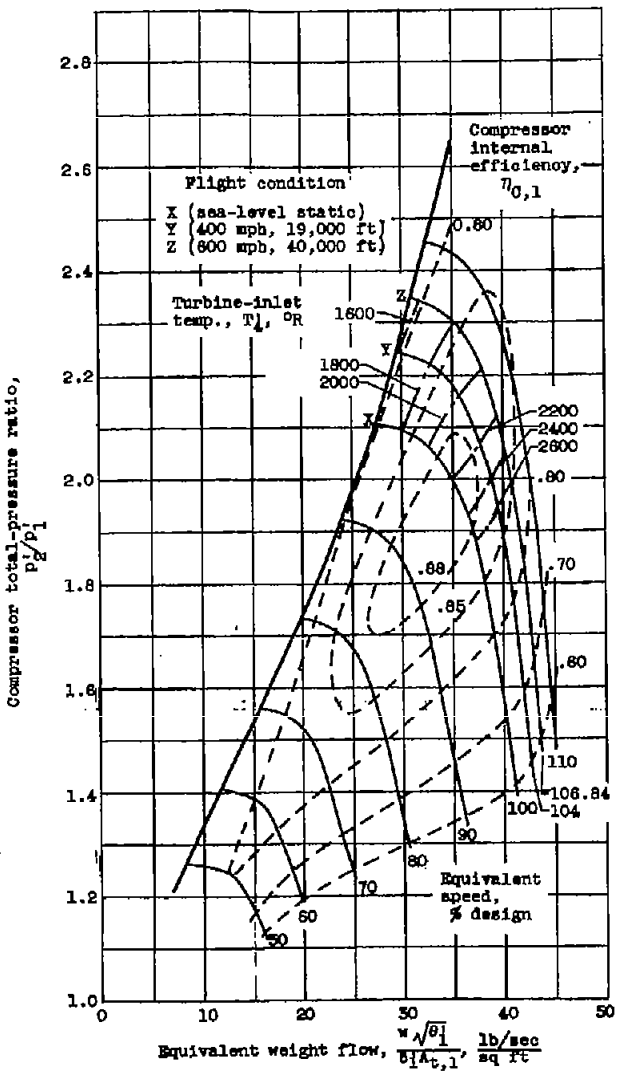

(e) Compressor-pressure-ratio split, 2-8; outer compressor.

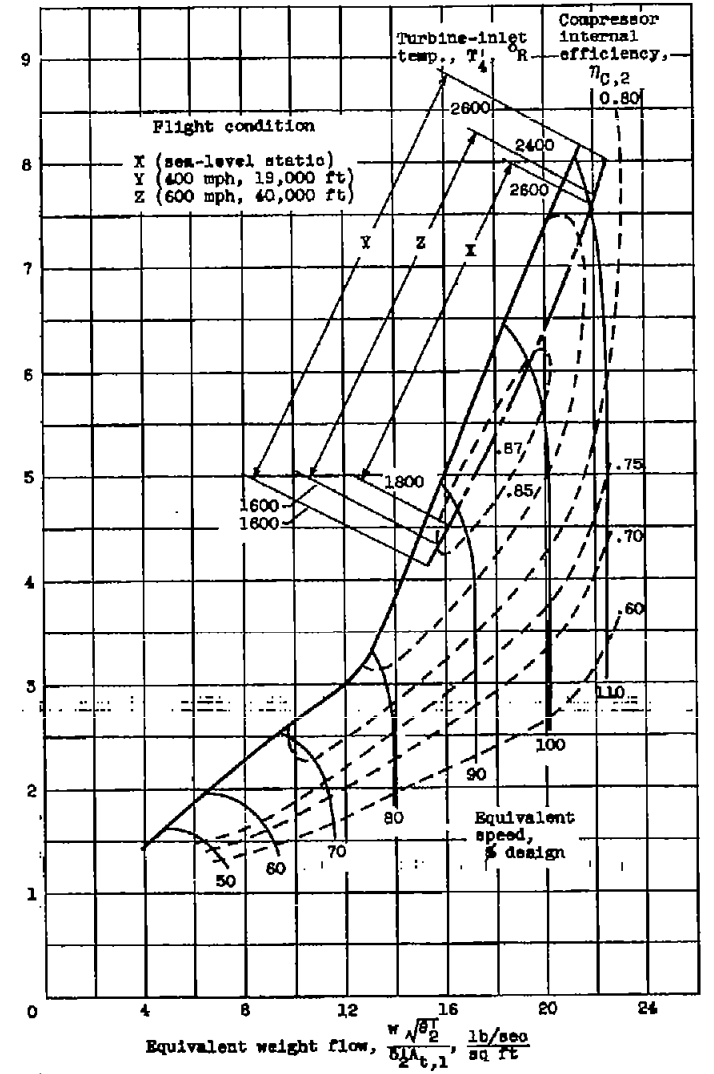

(f) Compressor-pressure-ratio split, 2-6; inner compressor.

Figure 2. - Concluded. Compressor performance maps.

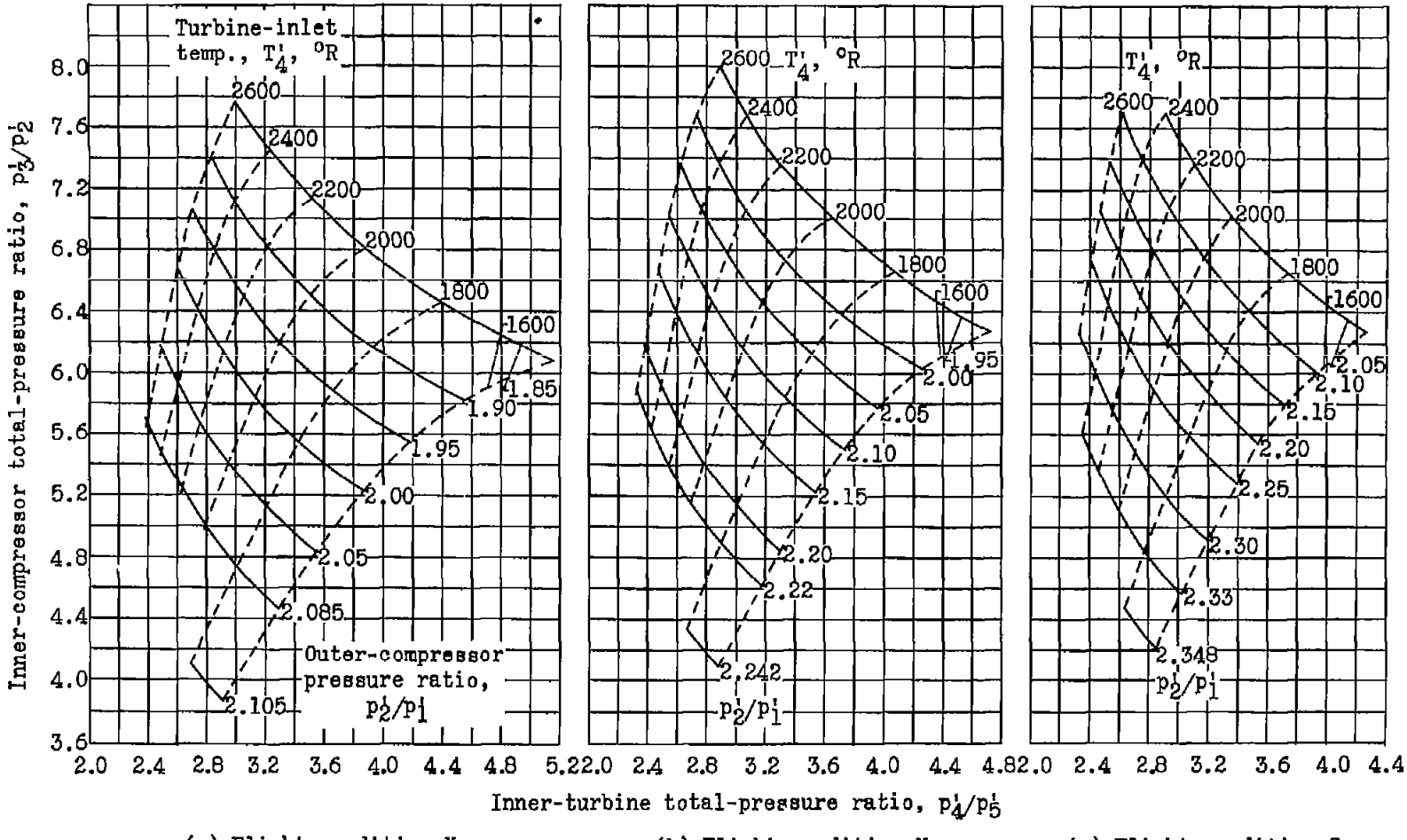

(a) Flight condition X. (b) Flight condition Y. (c) Flight condition Z.

Figure 3. - Variation of compressor pressure ratios with turbine-inlet temperature and inner-turbine pressure ratio for 2-6 engines.

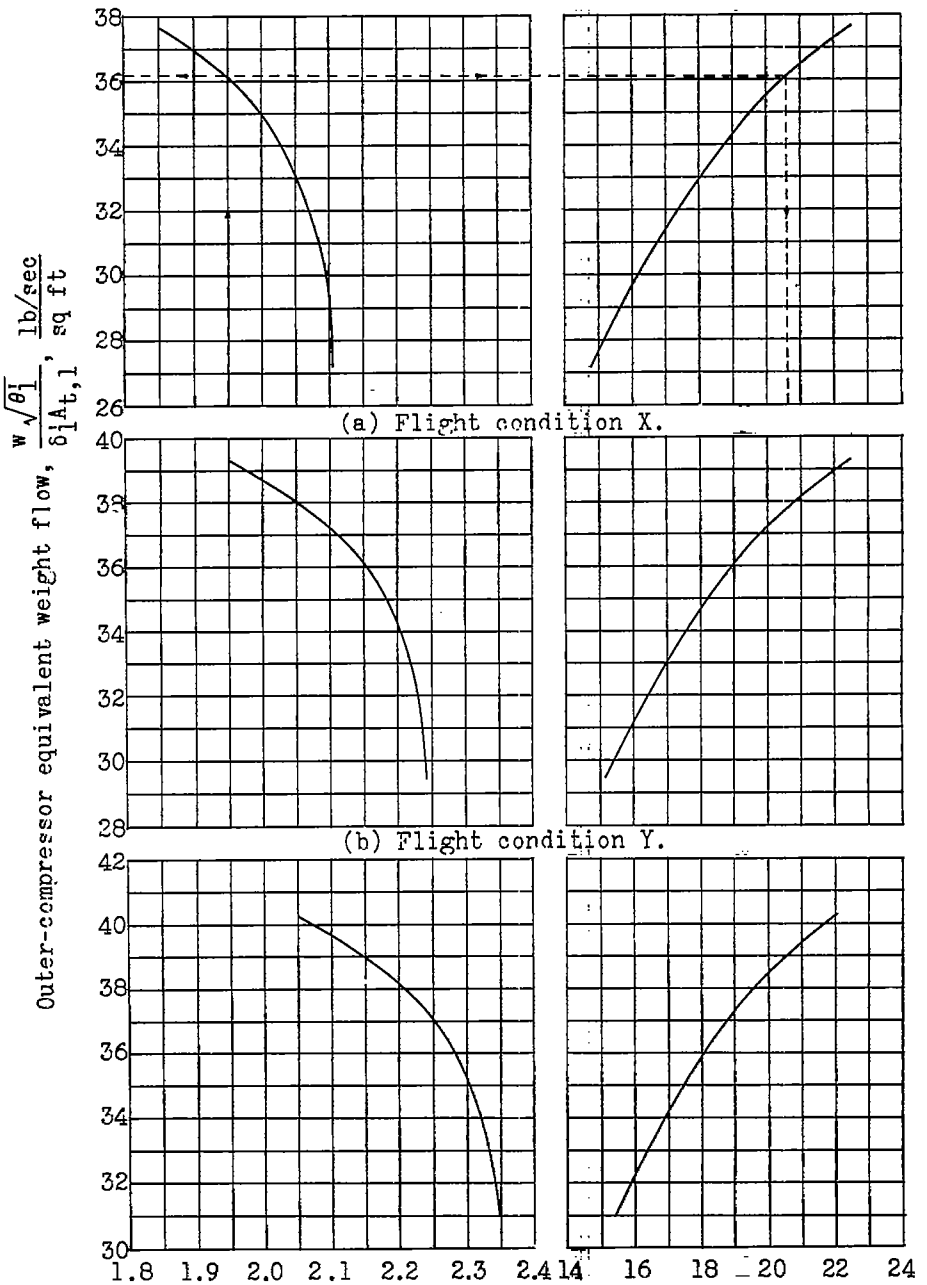

(c) Flight condition Z.

Figure 4. - Variation of compressor equivalent weight flows with outer-compressor pressure ratio for 2-6 engines.

[redacted]

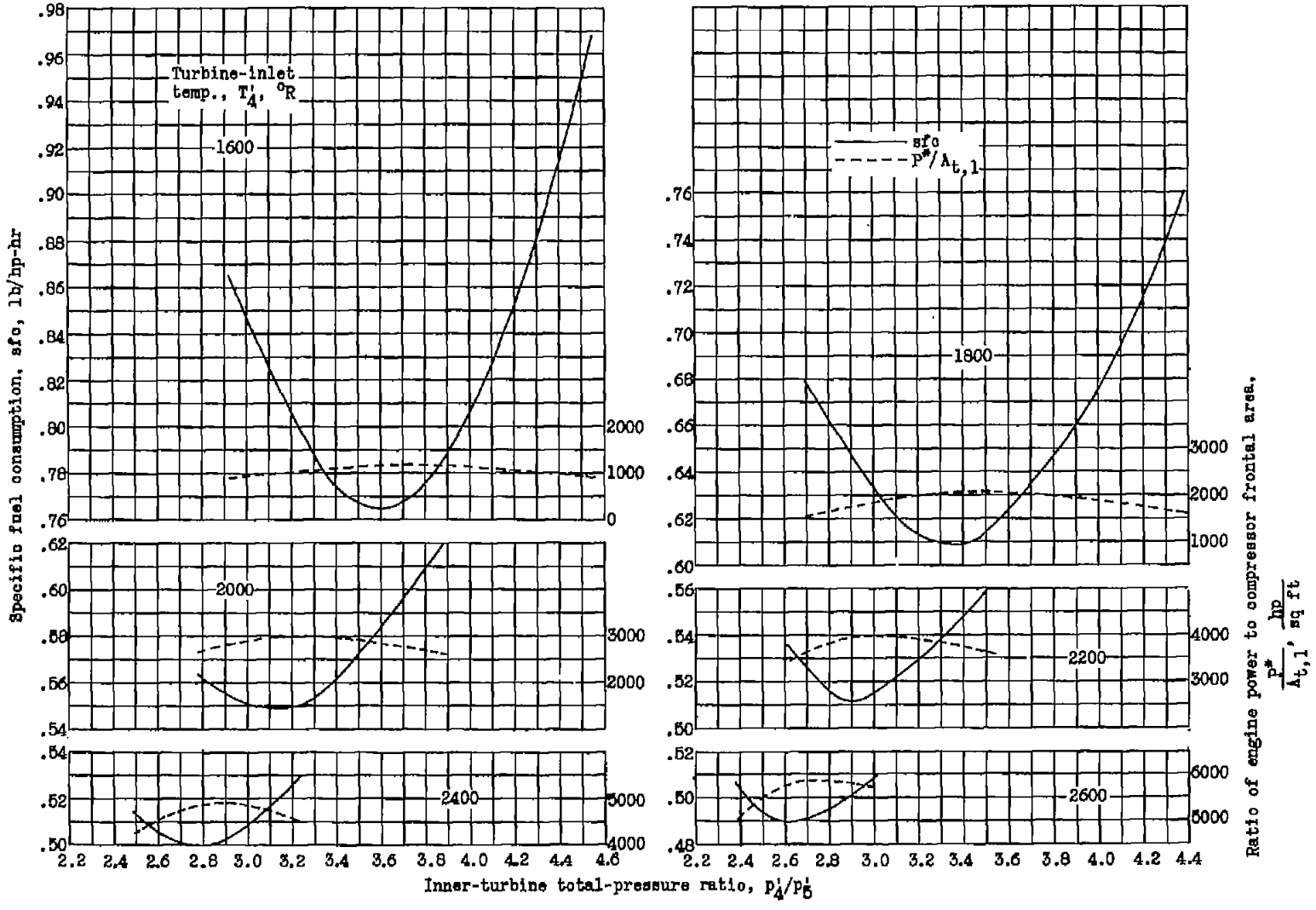

(a) Flight condition X.

Figure 5. - Variation of engine power and specific fuel consumption with turbine-inlet temperature and inner-turbine pressure ratio for 2-6 engines.

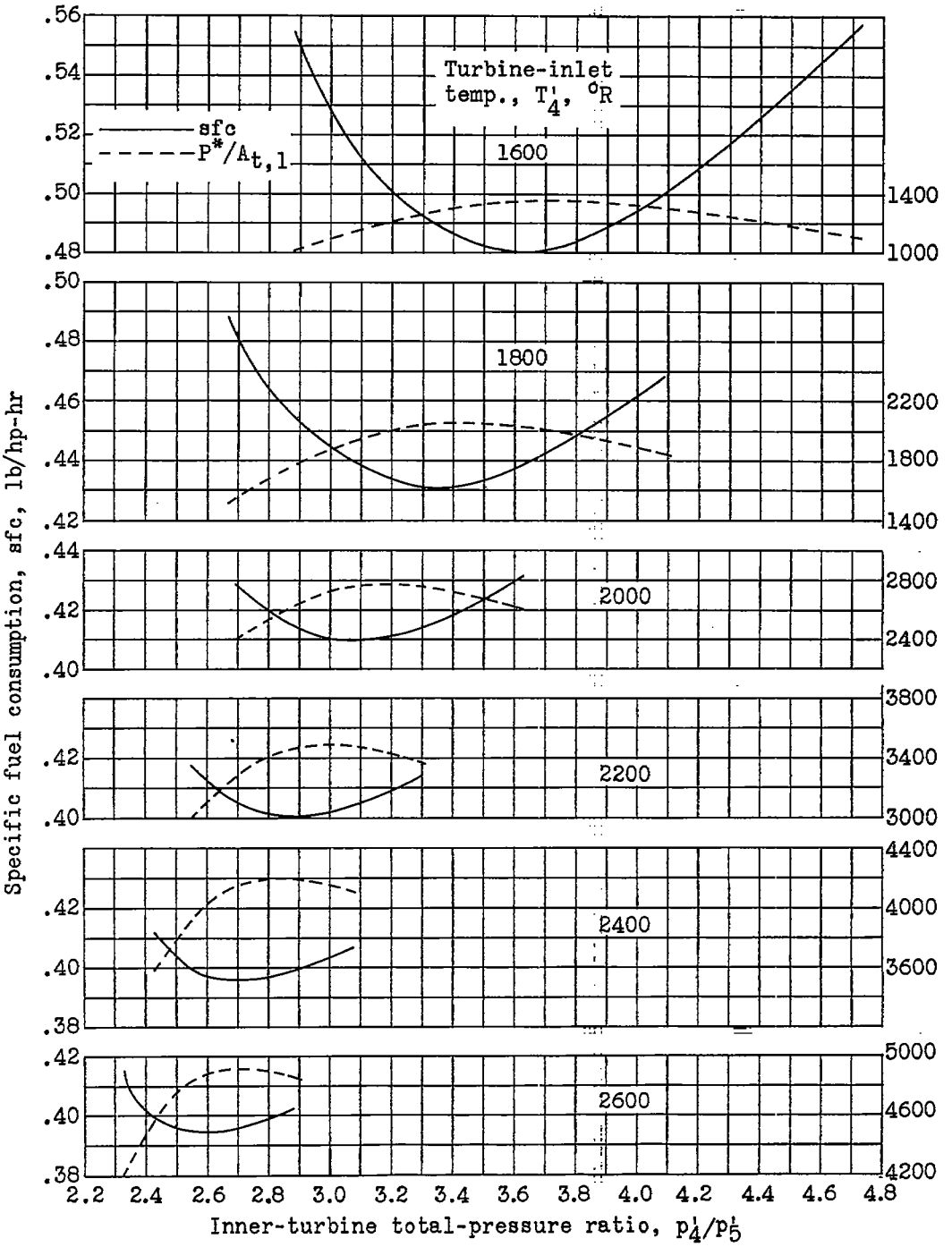

(b) Flight condition Y.

Figure 5. - Continued. Variation of engine power and specific fuel consumption with turbine-inlet temperature and inner-turbine pressure ratio for 2-6 engines.

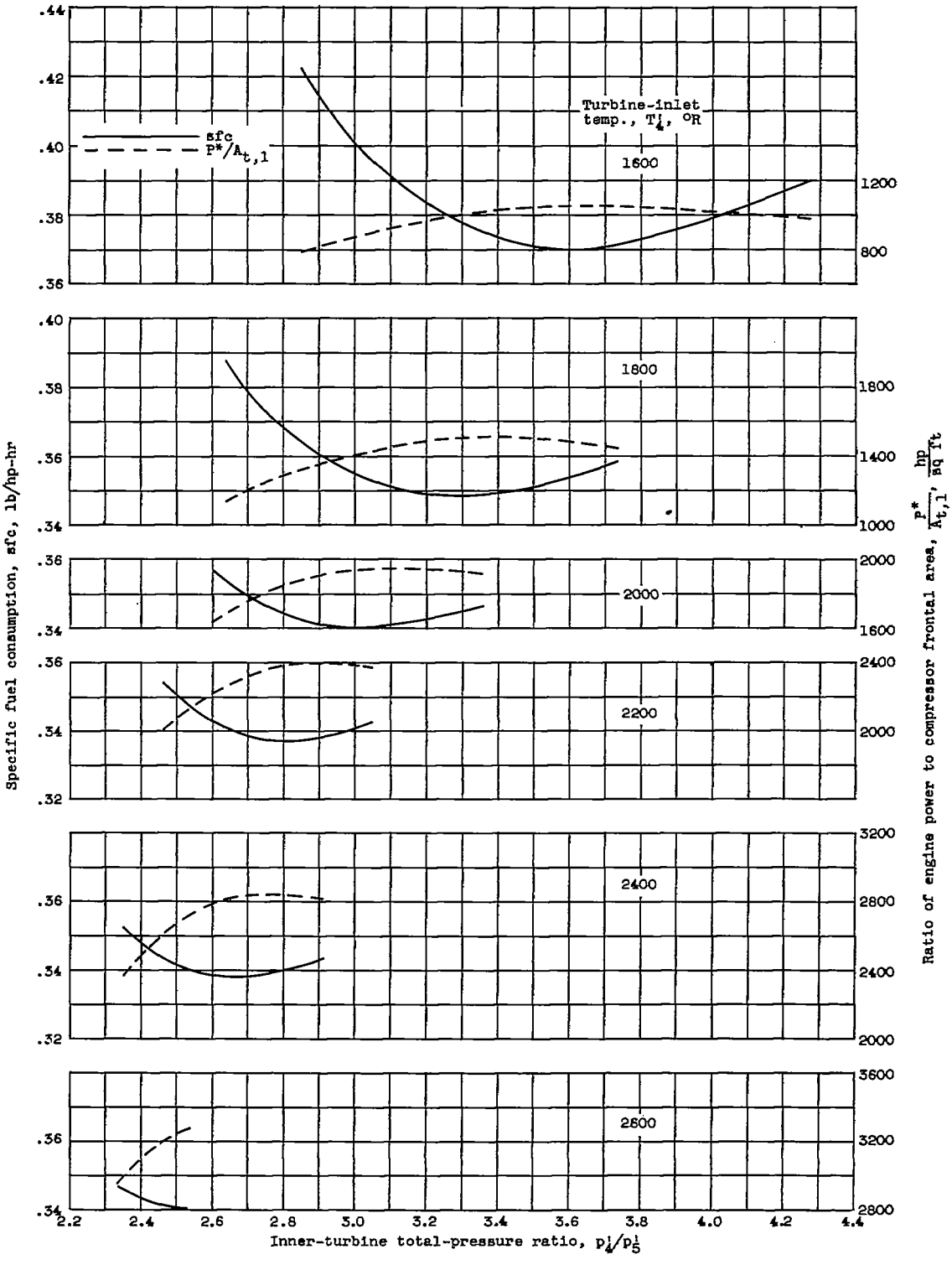

(c) Flight condition Z.

Figure 5. - Concluded. Variation of engine power and specific fuel consumption with turbine-inlet temperature and inner-turbine pressure ratio for 2-6 engines.

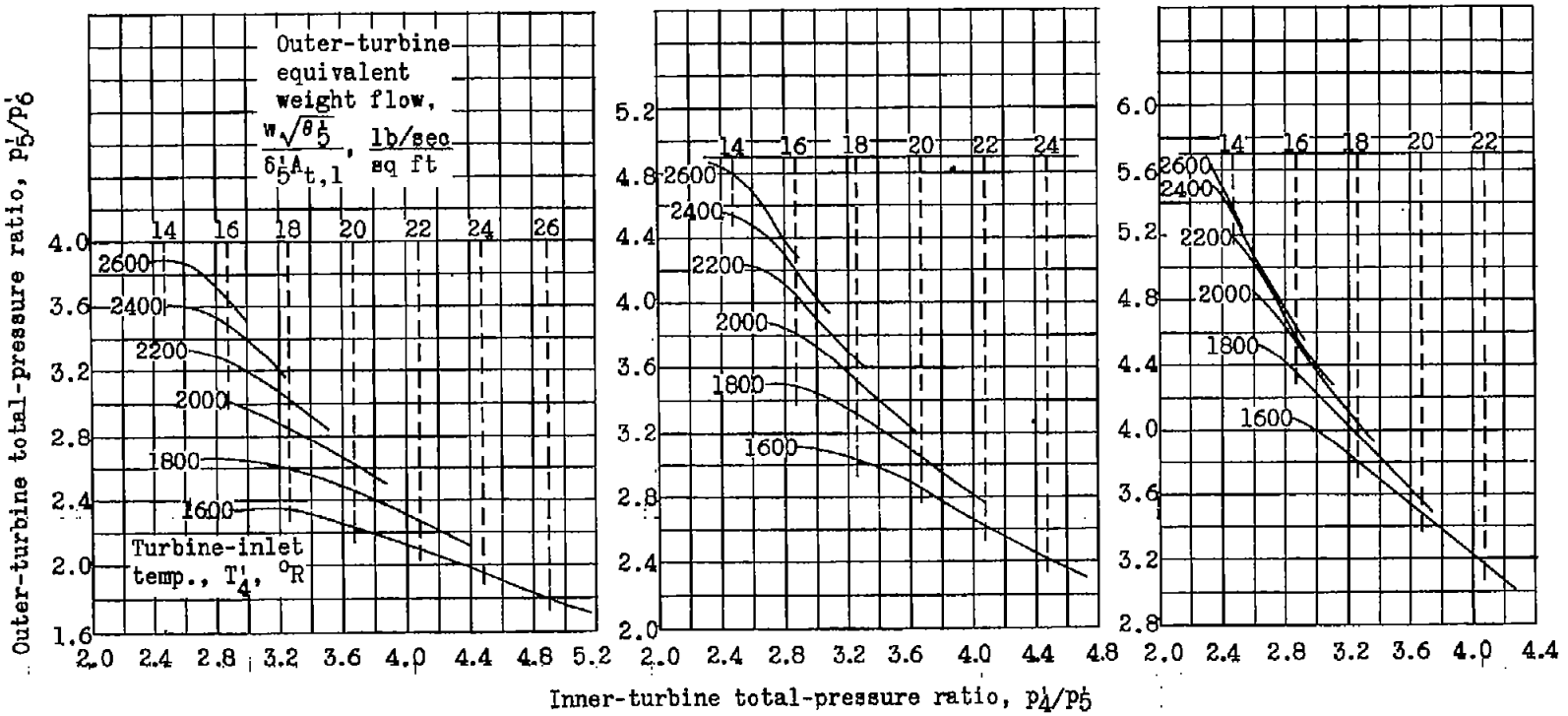

(a) Flight condition X. (b) Flight condition Y. (c) Flight condition Z.

Figure 6. - Variation of outer-turbine pressure ratio and equivalent weight flow with turbine-inlet temperature and inner-turbine pressure ratio for 2-6 engines.

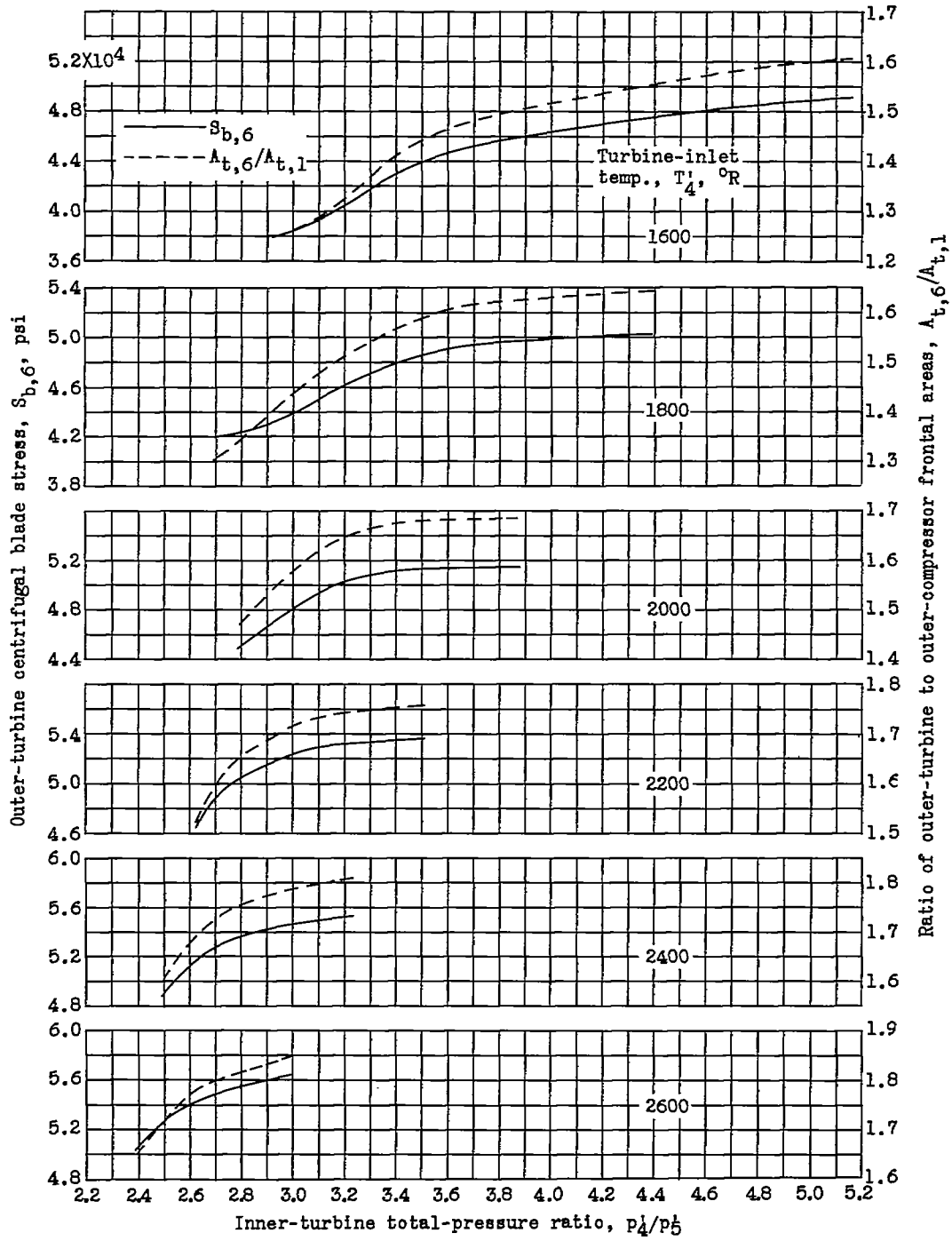

(a) Flight condition X.

Figure 7. - Variation of outer-turbine frontal area and blade stress with turbine-inlet temperature and inner-turbine pressure ratio for 2-6 engines.

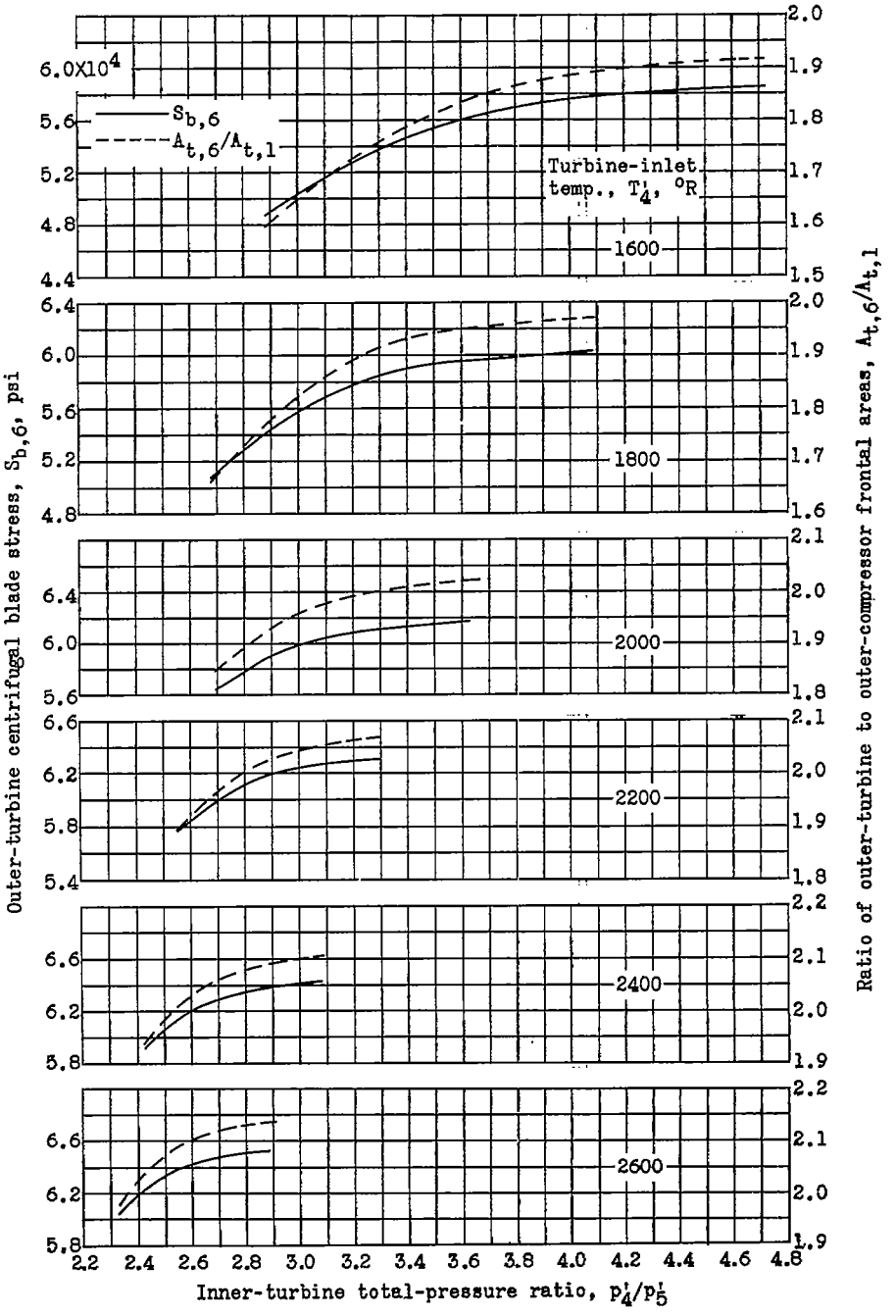

(b) Flight condition Y.

Figure 7. - Continued. Variation of outer-turbine frontal area and blade stress with turbine-inlet temperature and inner-turbine pressure ratio for 2-6 engines.

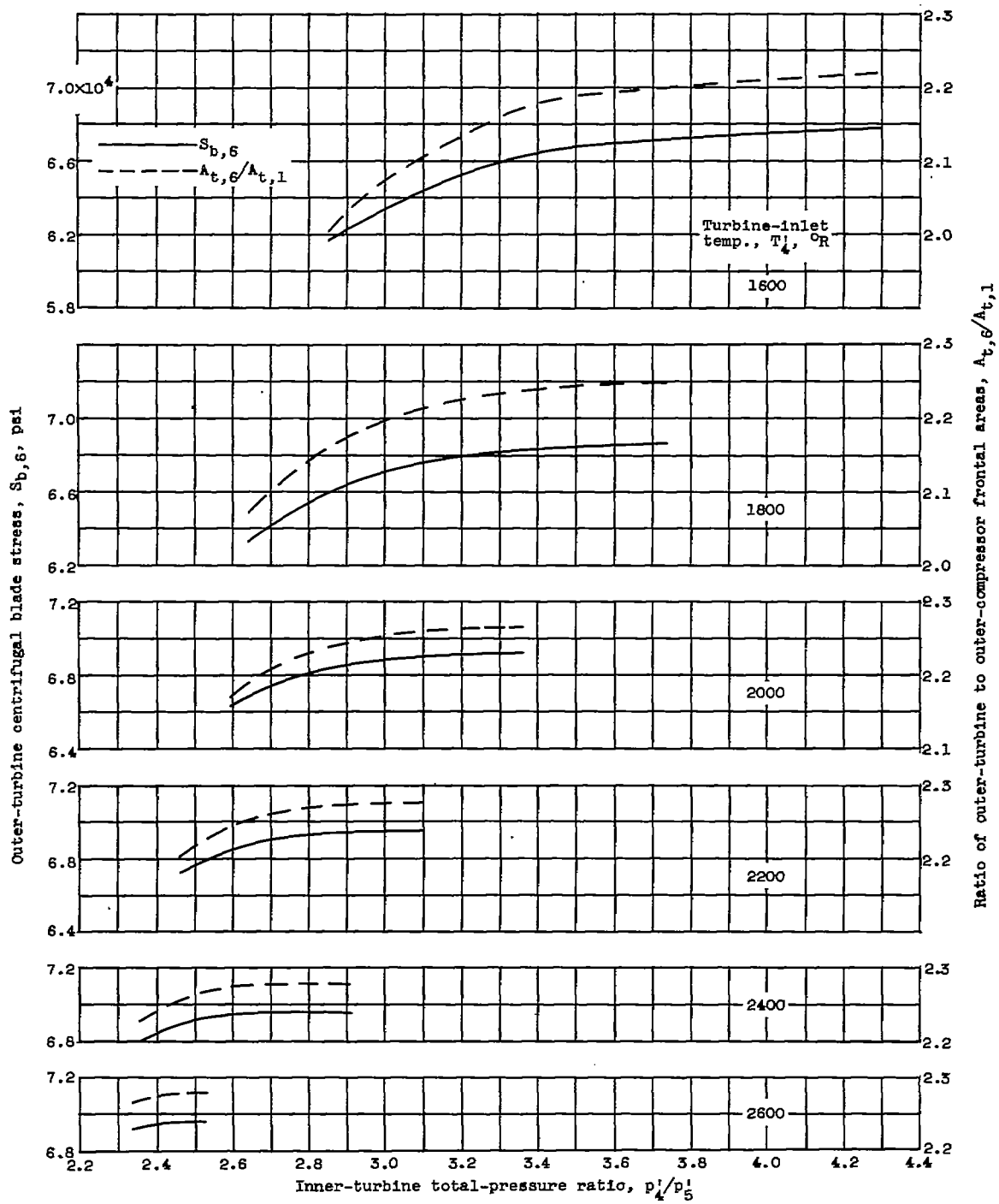

(c) Flight condition Z.

Figure 7. - Concluded. Variation of outer-turbine frontal area and blade stress with turbine-inlet temperature and inner-turbine pressure ratio for 2-6 engines.

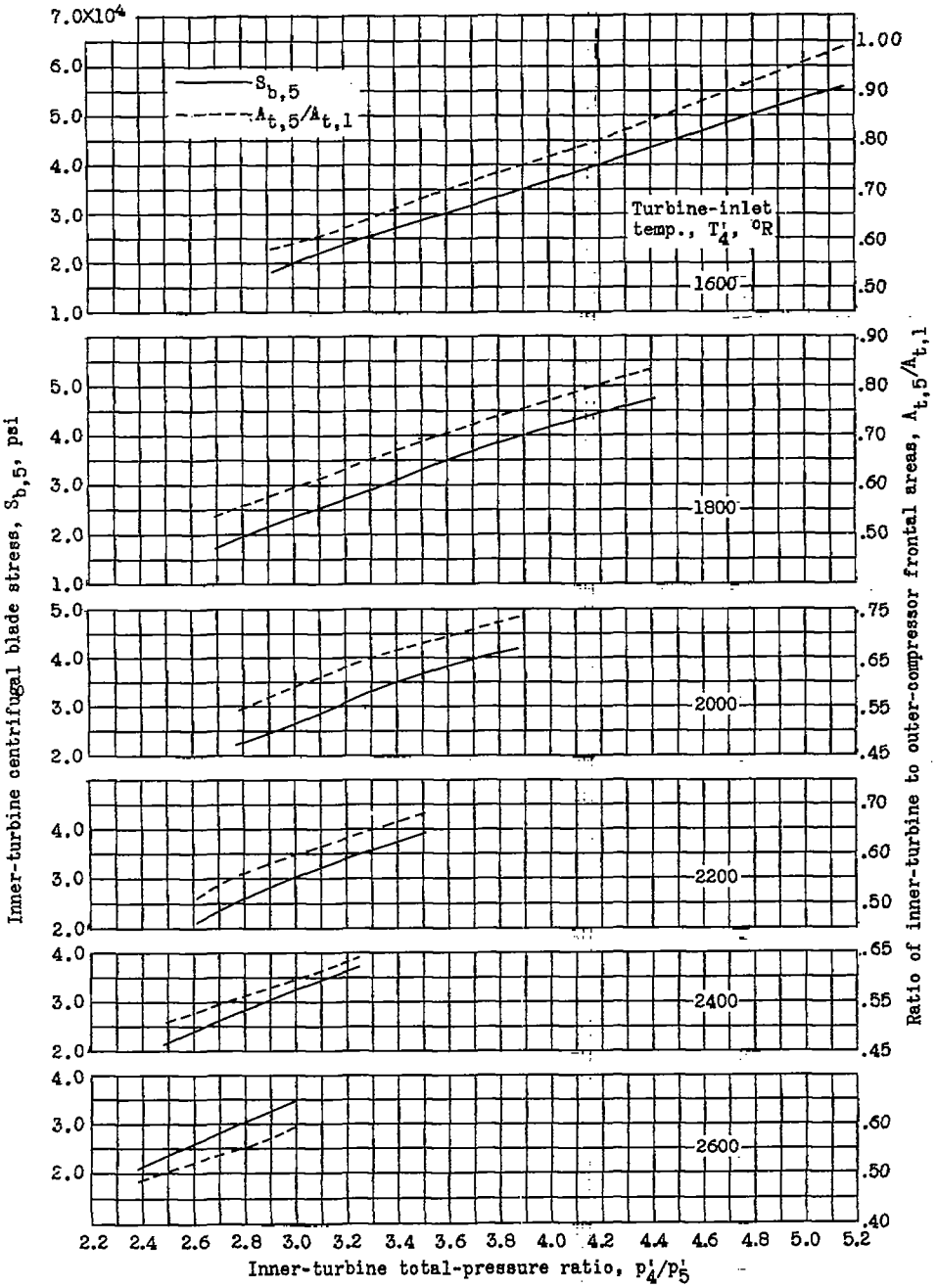

(a) Flight condition X.

Figure 8. - Variation of inner-turbine frontal area and blade stress with turbine-inlet temperature and inner-turbine pressure ratio for 2-6 engines.

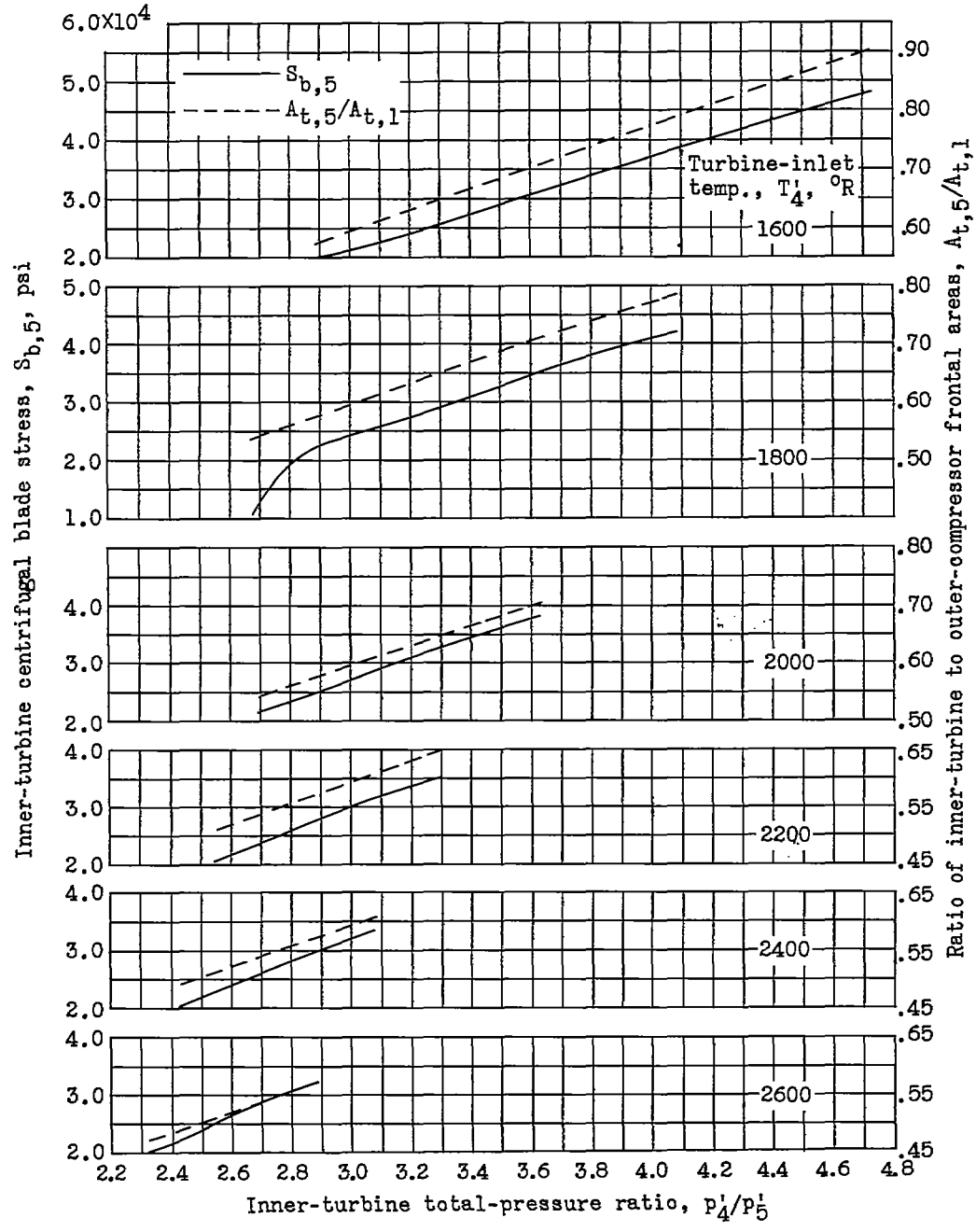

(b) Flight condition Y.

Figure 8. - Continued. Variation of inner-turbine frontal area and blade stress with turbine-inlet temperature and inner-turbine pressure ratio for 2-6 engines.

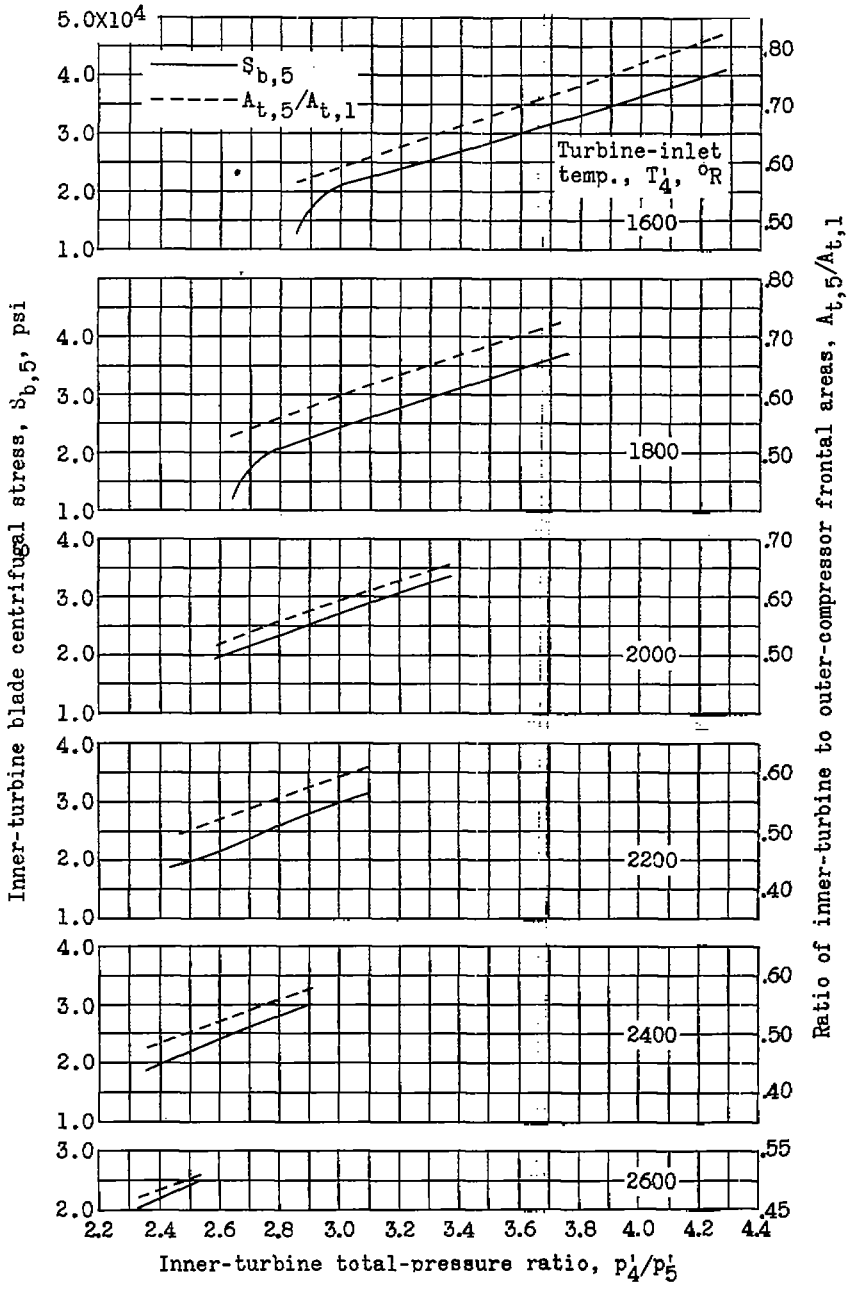

(c) Flight condition Z.

Figure 8. - Concluded. Variation of inner-turbine frontal area and blade stress with turbine-inlet temperature and inner-turbine pressure ratio for 2-6 engines.

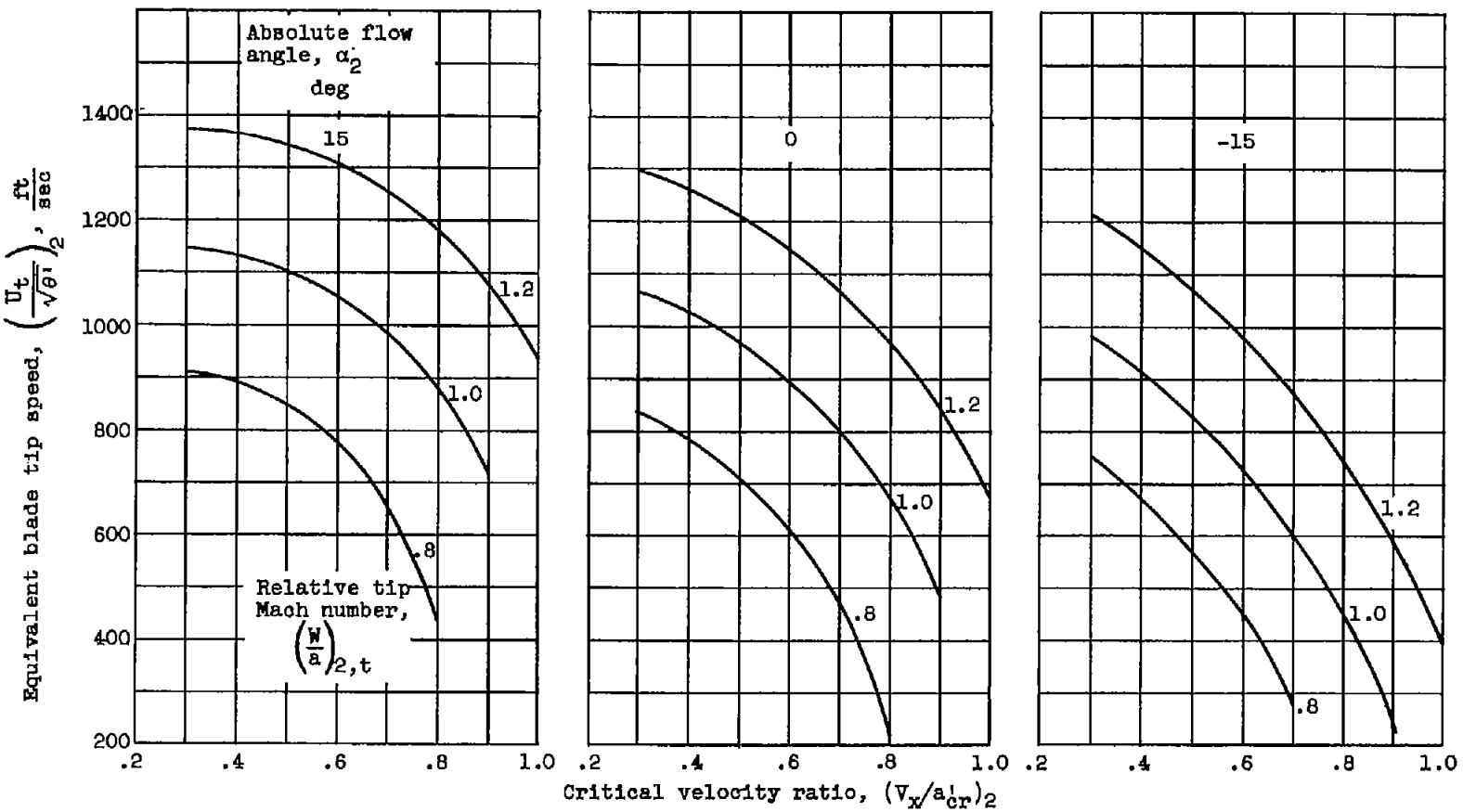

(a) Inner-compressor tip speed.

Figure 9. - Selection of aerodynamic and geometric parameters at sea-level static condition and turbine-inlet temperature of 2100° R.

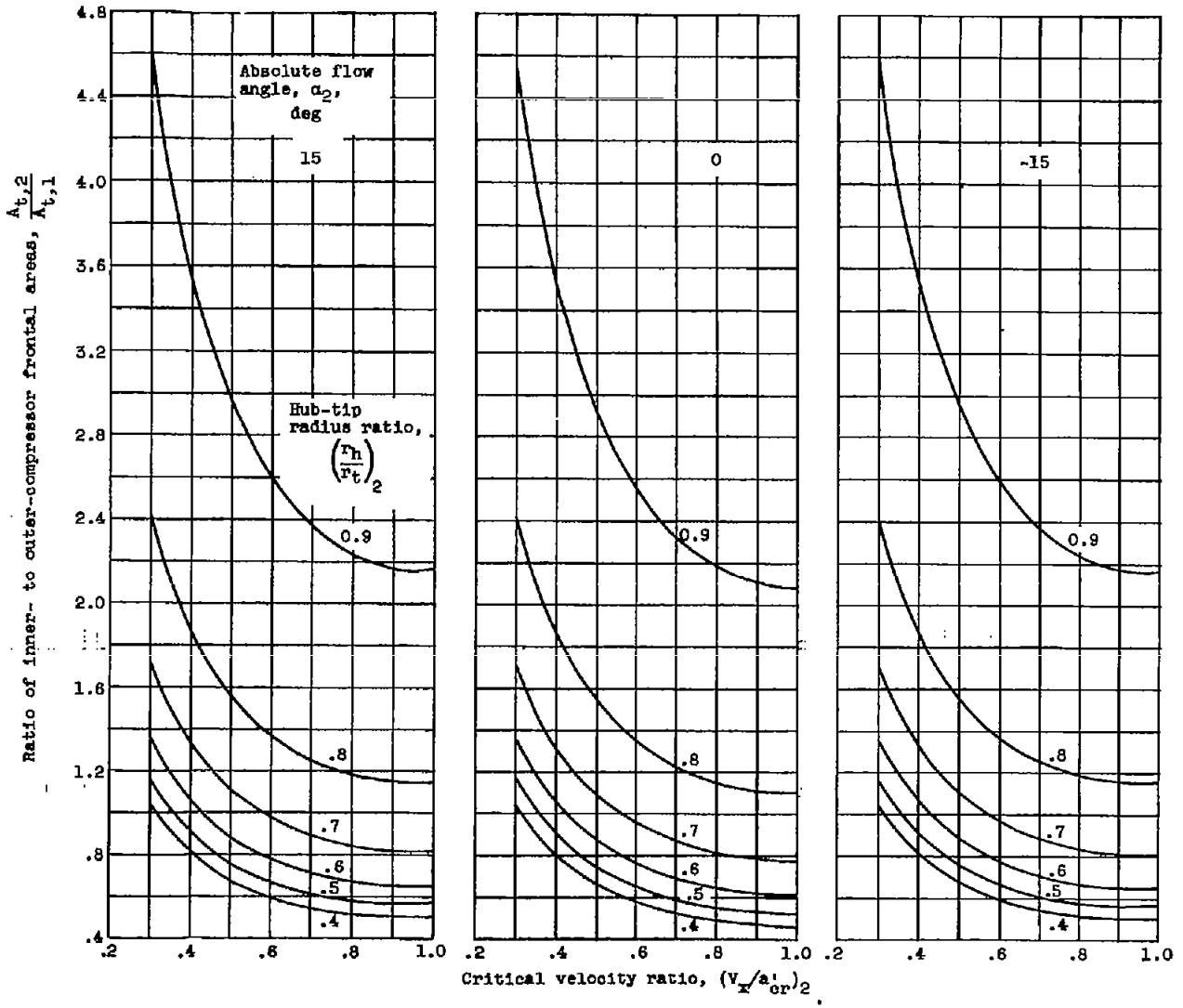

(b) Inner-compressor frontal area.

Figure 9. - Continued. Selection of aerodynamic and geometric parameters at sea-level static condition and turbine-inlet temperature of 2100° R.

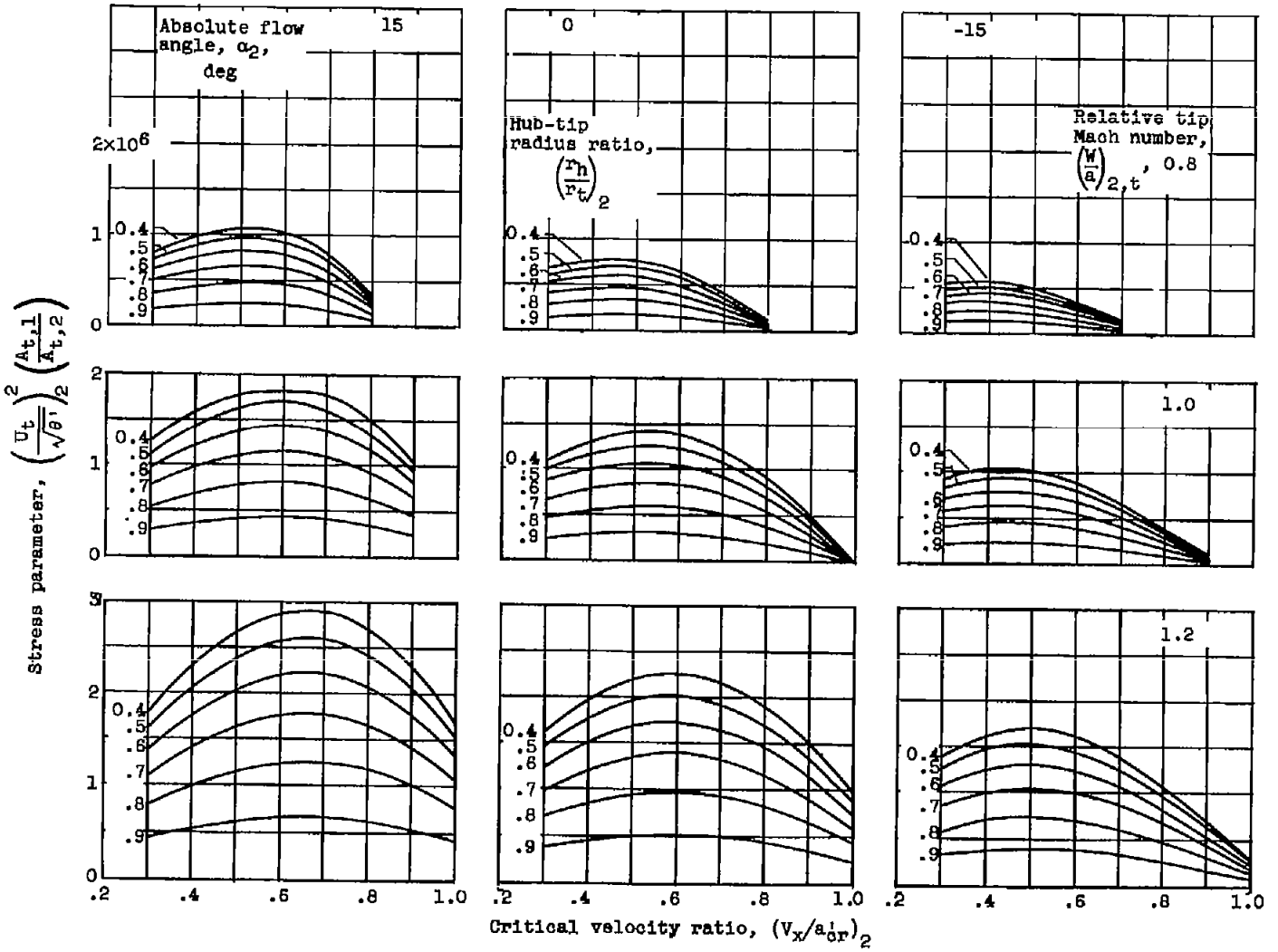

(c) Inner-compressor hub-tip radius ratio and absolute flow angle.

Figure 9. - Continued. Selection of aerodynamic and geometric parameters at sea-level static condition and turbine-inlet temperature of 2100° R.

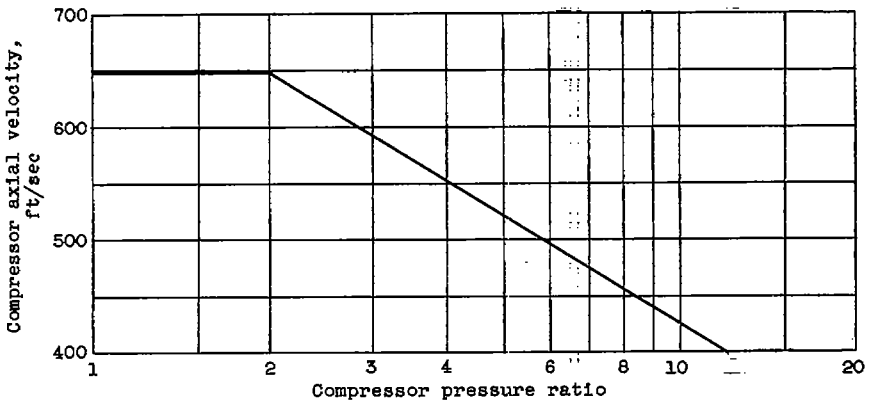

(d) Compressor axial velocity distribution.

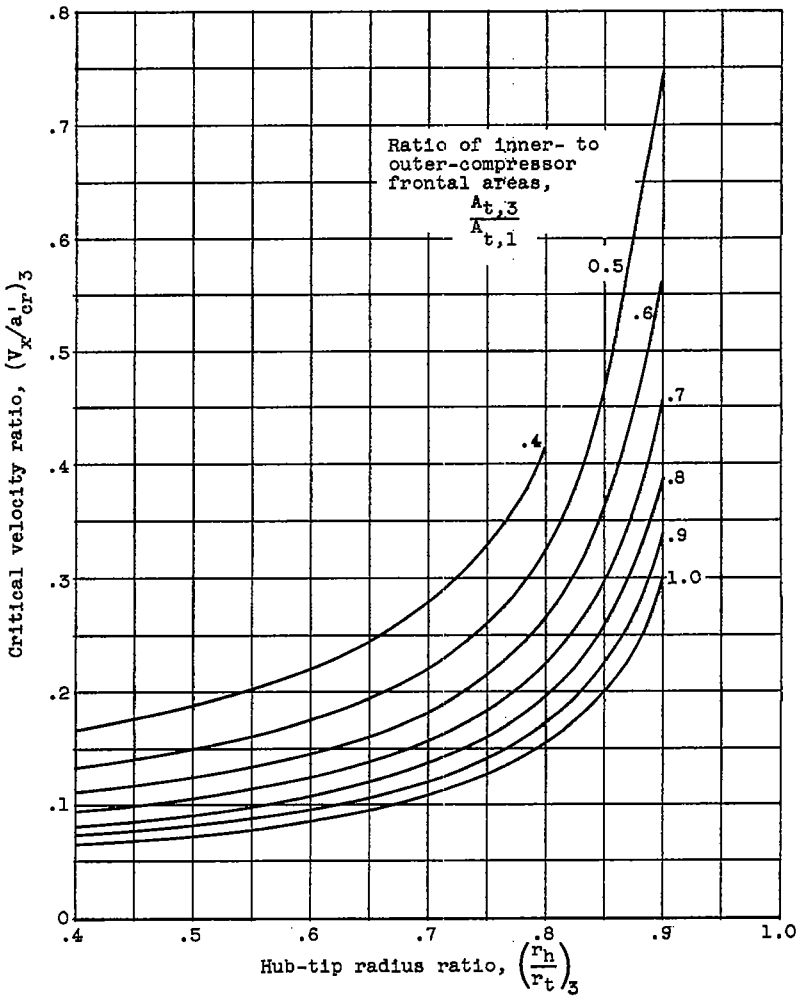

(e) Inner-compressor exit hub-tip radius ratio and frontal area.

Figure 9. - Continued. Selection of aerodynamic and geometric parameters at sea-level static condition and turbine-inlet temperature of 2100° R.

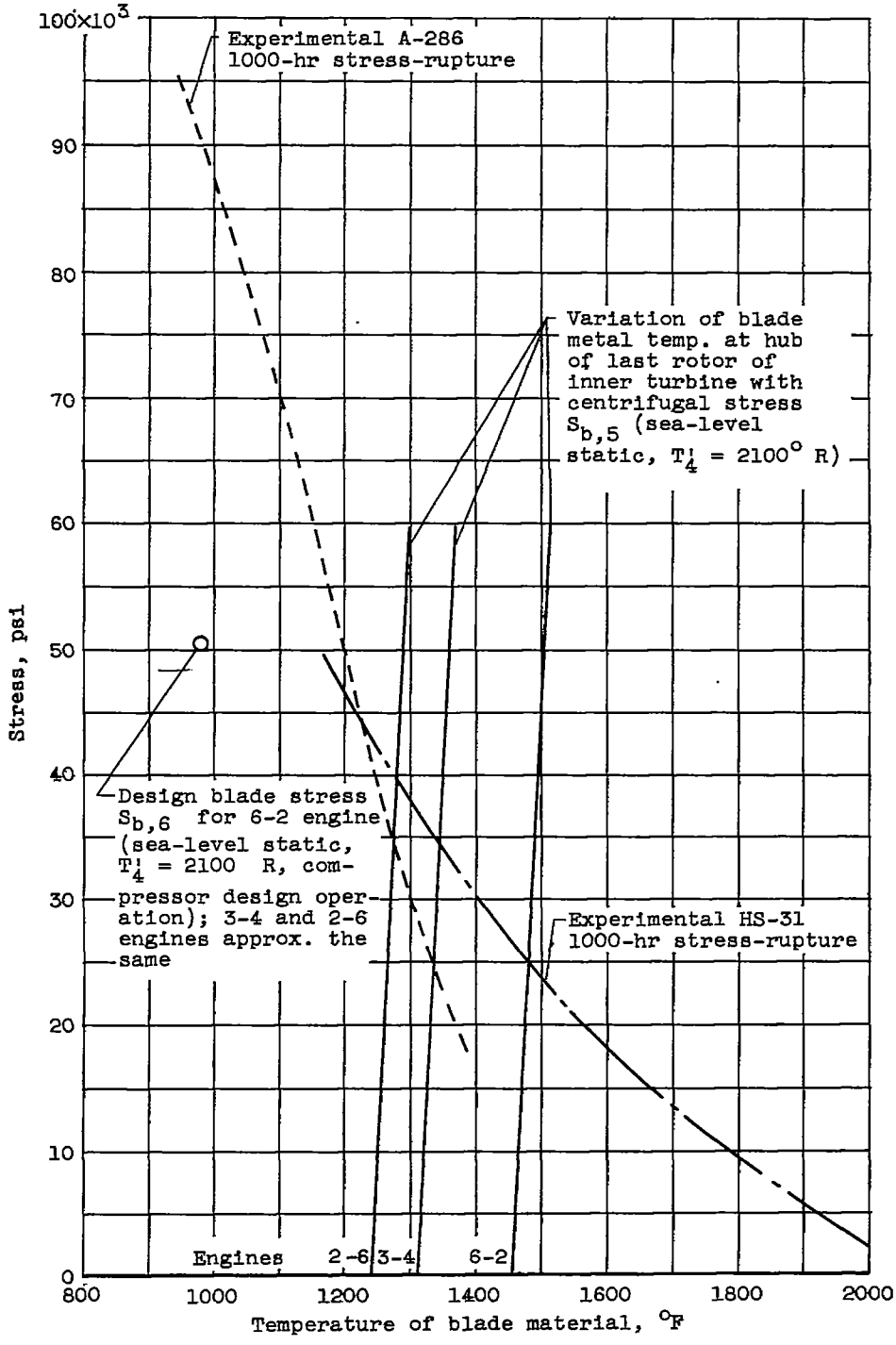

(f) Inner-turbine allowable stress.

Figure 9. - Concluded. Selection of aerodynamic and geometric parameters at sea-level static condition and turbine-inlet temperature of 2100° R.

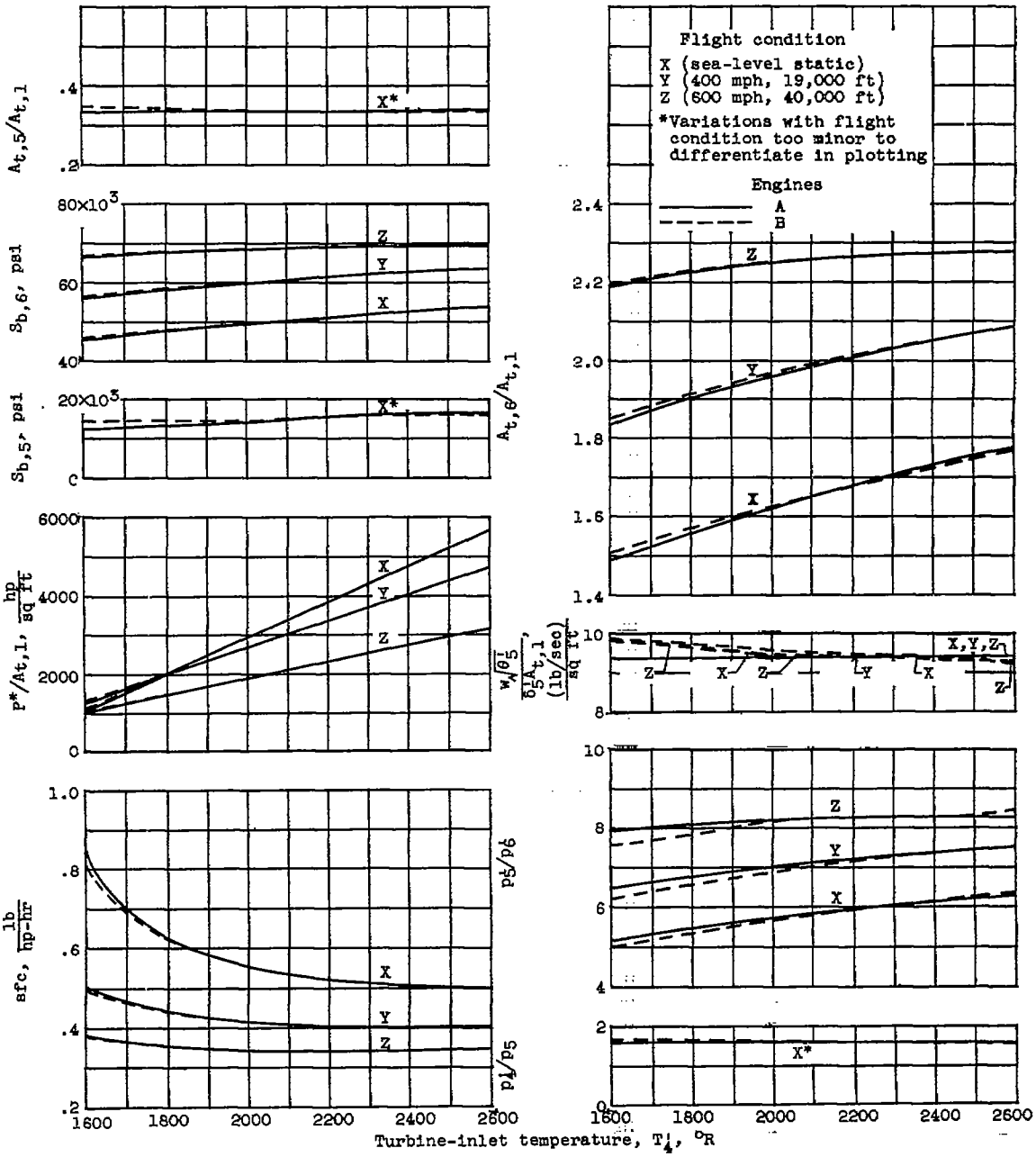

(a) Compressor-pressure-ratio split, 6-2.

Figure 10. - Variation of engine design parameters and operating conditions with turbine-inlet temperature and flight condition.

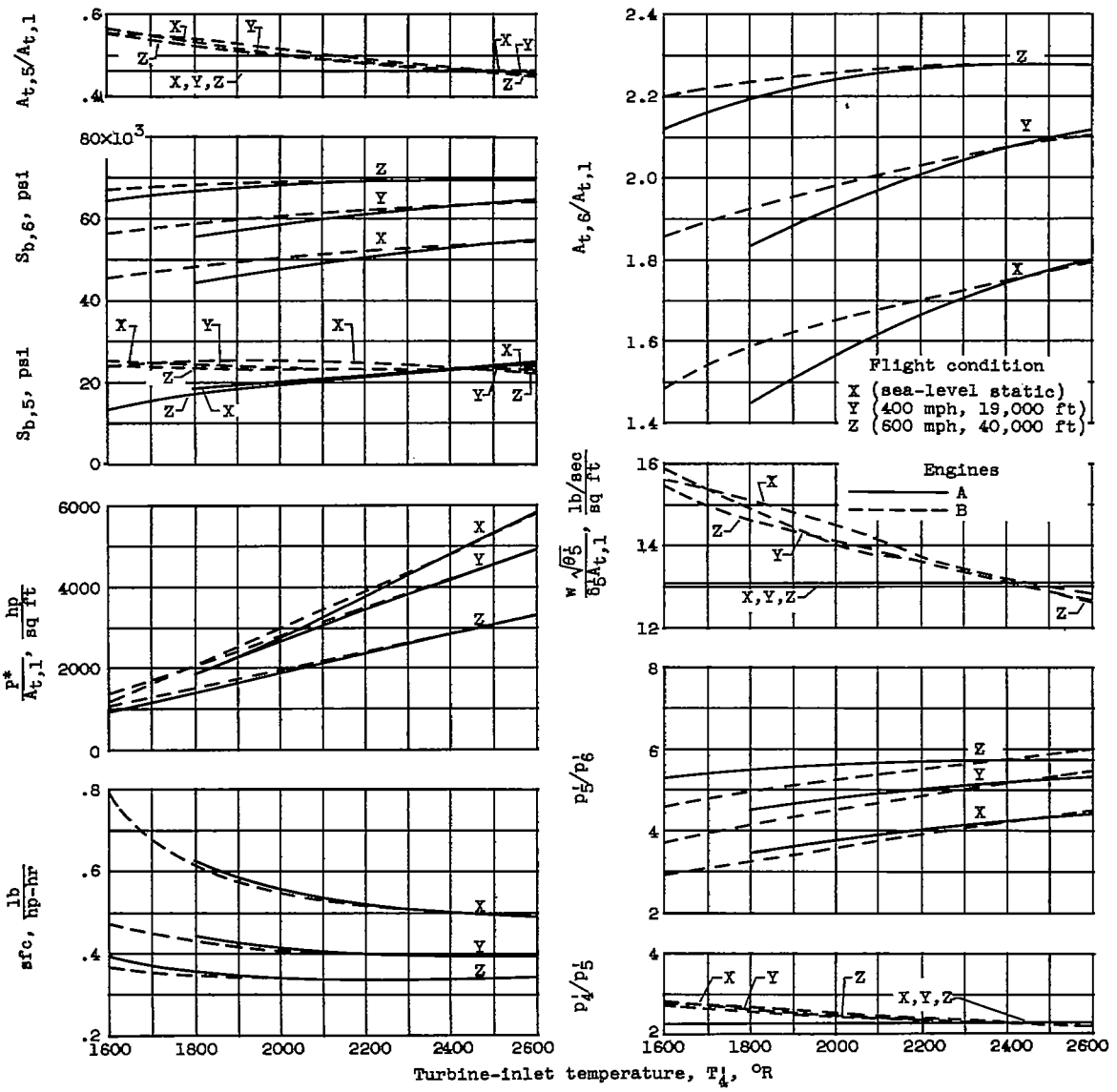

(b) Compressor-pressure-ratio split, 3-4.

Figure 10. - Continued. Variation of engine design parameters and operating conditions with turbine-inlet temperature and flight condition.

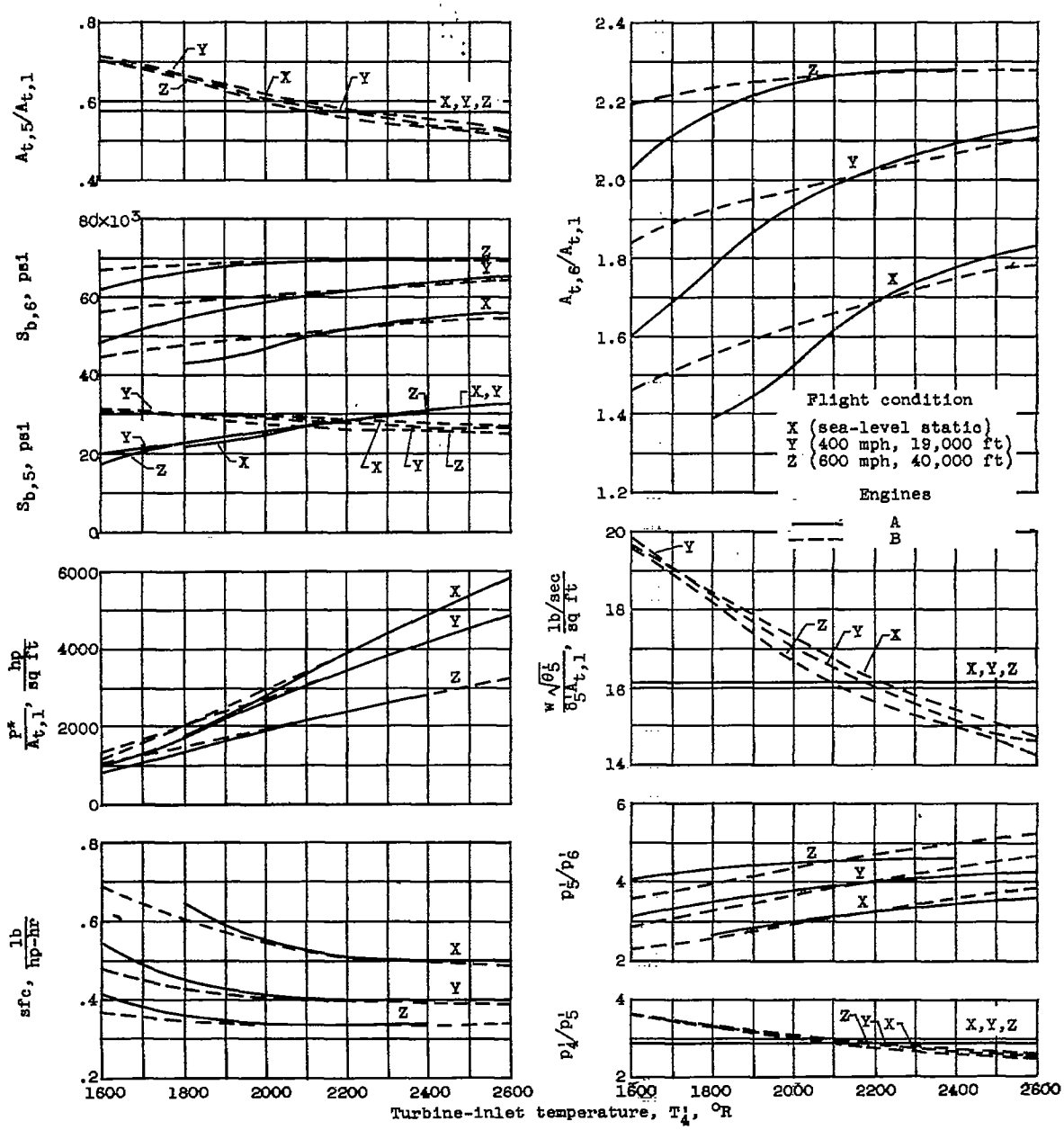

(c) Compressor-pressure-ratio split, 2-6.

Figure 10. - Concluded. Variation of engine design parameters and operating conditions with turbine-inlet temperature and flight condition.